**THERMAL CHARACTERISTICS OF PITCH BASED
CARBON FOAM AND PHASE CHANGE
MATERIALS**

THESIS

Kevin Wierschke, Captain, USAF

AFIT/GSS/ENY/05-M05

**DEPARTMENT OF THE AIR FORCE
AIR UNIVERSITY**

AIR FORCE INSTITUTE OF TECHNOLOGY

Wright-Patterson Air Force Base, Ohio

AFIT/GSS/ENY/05-M05

THERMAL CHARACTERISTICS OF PITCH BASED CARBON FOAM AND PHASE
CHANGE MATERIALS

THESIS

Presented to the Faculty

Department of Aeronautical and Astronautical Engineering

Graduate School of Engineering and Management

Air Force Institute of Technology

Air University

Air Education and Training Command

In Partial Fulfillment of the Requirements for the

Degree of Master of Science in Astronautical Engineering

Kevin W. Wierschke, BS

Captain, USAF

March 2005

APPROVED FOR PUBLIC RELEASE; DISTRIBUTION UNLIMITED.

THERMAL CHARACTERISTICS OF PITCH BASED CARBON FOAM AND PHASE CHANGE MATERIALS

Kevin W. Wierschke, BS

Captain, USAF

Approved:

_____   9 Mar 05
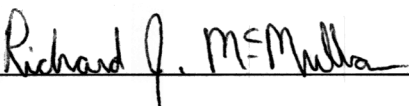
Dr. Milton Franke (Chairman)

_____   9 Mar 05

LtCol Eric Stephen

_____   9 Mar 05

Maj Richard McMullan

Abstract

The purpose of this thesis is to determine the transient response of carbon foam with a phase-change material by measuring the response of the pitch-based carbon foam and phase-change materials to a step temperature input. An analytic response was created and compared against the measured response.

These pitch-based carbon foams exhibit thermal conductivities along the ligaments of up to 1500 W/m-K with bulk thermal conductivities of 5-250 W/m-K.   This high thermal conductivity and porosity of up to 90% allows the possibility of infiltrating the foam with a relatively large volume of phase-change material.

Phase-change thermal energy storage devices offer thermal control systems an option that allows a smaller heat sink to be used by absorbing the thermal energy quickly and storing it in the phase change to prevent failure of electronic components and slowly releasing the heat to the heat sink.

The experiment applied step temperature inputs to test samples. The transient response was recorded until steady state was reached. Samples were prepared by bonding the foam to a carbon-carbon plate on both top and bottom and machining to size. The foam was infiltrated with the phase-change material and sealed with an epoxy resin.

By performing an energy balance an analytic prediction of the transient response was developed. This approximation was then compared to the experimental results.

To my wife, for all her support

Acknowledgments

I would like to express my sincere appreciation to my faculty advisor, Prof Milton Franke, for his guidance and support throughout the course of this thesis effort. The insight and experience was certainly appreciated. I would also like to thank my sponsor, Roland Watts, from the Air Force Research Lab for both the support and latitude provided to me in this endeavor. Finally I would like to thank Dr. Rengasamy Ponnappan for his guidance and support.

Kevin W. Wierschke

Table of Contents

List of Figures

List of Tables

Page

Nomenclature

A	Area
c	Specific heat
E	Energy
E_{stored}	Energy stored
$\dot{E}$	Time derivative of Energy
h_{sf}	Latent heat of fusion
k	Thermal conductivity
L	Length
M	Mass
q	Heat flux
R	Thermal resistance
T	Temperature
t	time
θ	Temperature difference between hot boundary condition and foam
τ	time constant

Subscripts

C	the cold side
f	foam
H	the hot side
in	into the region being considered
out	out of the region being considered
PCM	phase-change material

THERMAL CHARACTERISTICS OF PITCH BASED CARBON FOAM AND PHASE CHANGE MATERIALS

I. Introduction

Background

Thermally conductive carbon foam is showing great promise as a new material improving the thermal management systems for space and airborne applications. Its characteristics of high thermal conductivity, low density, and high porosity makes it ideal to use in situations where copper is unsuitable. The high porosity forces the question: can the foam be filled with a phase change material? By doing so, a thermal energy storage system would be created. This energy storage system is ideal for short duty cycle, high power applications or applications with oscillatory heat loading. These applications could be as widely varied as burst lasers, thermal protection for spacecraft reentry, or even power amplifiers used in communications systems.

Carbon foam derived from a blown mesophase pitch precursor can be considered to be an interconnected network of graphitic ligaments (11:29). These foams consist of an open cell structure that allows fluids to flow through easily. This foam is created through a process of heating and pressurization cycles of pitch (9:1-2).

1

Phase-change materials have been in use for temperature regulation by NASA as far back as the lunar rover (6:1-1) because of their ability to absorb thermal energy while maintaining a nearly constant temperature during the phase change; therefore, creating a lower the system temperature for a short period of time compared with a system without phase-change materials. Hale, in *Phase Change Materials Handbook*, defined the ideal phase-change material as having the following characteristics:

- High heat of fusion
- Reversible solid to liquid transition
- High Thermal conductivity
- High Specific Heat and density
- Long term reliability during repeated cycling
- Dependable freezing behavior
- Low volume change during phase transition
- Low vapor pressure (6:1-1)

The carbon foam with its small pore size and high thermal conductivity allows the selection of phase-change materials without much consideration of the phase-change material's thermal conductivity, as the carbon foam will distribute the heat within the phase-change material. Therefore, the system should be an excellent thermal energy storage device.

Problem Statement

During the course of this experiment the primary purpose is to investigate the transient thermal characteristics of the carbon foam with an infiltrated phase-change material. This is performed by looking at the time constant of the transient response and the phase change duration, and comparing to an analytical model. Secondary goals are

the investigation of methods to bond carbon-carbon plates to the carbon foam and to investigate the infiltration methods of the phase-change material.

Methodology

In order to determine the transient system performance, a transient heat load was applied. This transient load was given in such a way that the thermal response of the system would be observed. A step input was given to the test sample to observe the temperature response. This response curve was expected to appear as an exponential curve, first order response, with a temperature plateau during the phase change. This exponential curve can be described by the time constant, the rate at which the system increases in temperature, and the duration of the phase change, the length of the plateau. These two parameters, along with the knowledge of the boundary conditions, can provide enough information about the response to reproduce the approximate response of the foam.

Variations to the experiment were performed to investigate how these changes affect the response. Samples of foam were tested with different pore sizes and densities. Samples with no phase change materials were tested and with different phase-change materials.

Assumptions and Limitations

All calculations assume a one-dimensional heat flow in this thesis. This assumption was made because the sample is the same size as the heat focusing block and cold plate and the sample is insulated on the four other sides during the test. Second, in the predicted results section the carbon foam was assumed to be isothermal. This was considered to be a valid assumption because the lowest temperature measured in the foam was never more than 20% less than the highest temperature measurement of the foam at any particular time but usually was less than 10% less. Third, specific heat is assumed to remain constant over the temperature region considered. This was considered to be a valid assumption because the temperature region considered is small at a max temperature change in the test materials being 80° C.

II. Literature Review

Historical Perspectives

Thermal protection has been necessary since electronic devices have been in existence. In modern times, these devices are packed in smaller packages while at the same time consuming more power, therefore, making thermal protection more important. Many different methods have been created to keep these electronic systems from failing. Heat pipes move heat quickly across the length of the pipe utilizing a liquid/gas mixture and a wicking material. Heat exchangers transfer heat from one fluid to another. Heat sinks dump heat from an electronic chip to the ambient air. In some cases these components are combined to create more complex systems to remove heat. With new materials and methods to build these thermal protection systems, electronic systems can function effectively while producing more heat without failing.

Carbon Foam Construction

Pitch-based carbon foam is created by starting with pitch. The pitch is pressurized, saturated with gas and then heated. As the pressure is released, the pitch grows into foam. The foam is then stabilized in order to prevent its collapse, by heating in air at temperatures ranging between 170 °C and 250 °C (9:1-2). Stabilization is critical

in the proper formation of nodes and ligaments for high thermal conductivity (9:1-2).
The foam is carbonized and graphitized by heating again. Graphitization creates very
high thermal conductivity along each ligament of the foam that is on the order of 1500
W/mK (10:1) with bulk thermal conductivities varying between 5-250 W/mK. Carbon
foam provides this high thermal conductivity while having a density of only 0.016-0.8
g/cc. For comparison, oxygen-free copper has a thermal conductivity of 390 W/mK and
a density of 8.95 g/cc. Foam is machined using standard machine tooling and cuts easily
with a diamond saw. The foam readily wets many materials like paraffin and alcohols
but rejects water (12:1). These properties make carbon foam very attractive for use as a
component in thermal control systems where light weight is important.

Phase-Change Materials

Phase-change materials have been introduced into thermal control systems to aid
in the protection of transient loads by changing phase. This phase change absorbs the
heat energy, but instead of increasing in temperature, the material changes phase, either
by evaporation or melting. The phase-change materials can also keep systems warm by
releasing energy during a freezing or condensation phase change.

The amount of energy absorbed or released depends on the latent heat of fusion of
the specific material or the latent heat of vaporization depending on which phase change
transition is occurring. This is not, however, the only property that is important in
selection of a good phase-change material. Since most systems using phase change

6

materials are expected to have a long life, the reliability of the phase-change material properties during repeated phase-change cycling becomes an interesting factor to designers. All phase-change materials change volume during the phase change or with a change in temperature, but it is desirable for most applications to choose a phase change material where this volume change is minimal. High thermal conductivity of the phase-change material is desirable which allows the heat to spread evenly into the material and prevent temperature gradients in the phase-change material. Thermal conductivity is one of the properties that can be improved by infiltrating the phase-change material into a high conductivity lattice material such as metallic or carbon foam. A good starting point for selection of a phase-change material is Hale's *Phase-Change Materials Handbook*, which reviews many different possible phase-change materials.

Applications of phase-change materials in thermal control are varied. The Lunar rover and Skylab used phase-change materials (6:1-1). More recently, companies are building fabrics with phase-change materials for use in clothing. These fabrics are woven into gloves and jackets that can warm people who must spend time out in cold weather. Building construction is also taking advantage of these phase-change materials to conserve energy by reducing heating and cooling needs by placing the phase-change material in the walls and roofing of buildings the daytime heat can be stored to warm the structure in the night. The cool nighttime temperatures can be used to solidify the phase-change material and keep the structure cool in the daytime. More commonly pizza delivery bags are filled with phase change material, this material is heated before leaving the kitchen and maintains the pizza hot temperature during the delivery timeframe.

III. Methodology

Test Article Construction

Graphitized carbon foam, acquired from Poco Foam and MER Corporations. The MER Corporation's foam was less dense and had larger pore sizes than the Poco brand foam. This foam was cut to 5.6 cm x 3.8 cm x 2.5 cm, with the vertical direction of the foam being in the 2.5 cm dimension. The cutting was performed on a high-speed water-cooled diamond saw. The samples were washed and dried in distilled water to remove any carbon dust or other residue that might prevent good infiltration or bonding. K-800 UNI carbon-carbon composite plates were cut using the same process, for bonding on the top and bottom of the sample.

The bond was created using Aremco graphitic bonding material RM-551 which creates a 75% graphite 25% phenolic resin bond between the foam and each composite plate. The bond was cured using the recommended curing cycle of 2 hours at 80 F, 4 hours at 265 F, and 2 hours at 500 F. After the bond was completed it was inspected under a microscope for thickness and consistency. The bonds used in the test samples averaged approximately 0.025 cm thick. Thinner bonds were created; however, they failed under a slight loading.

The temperature of the foam was determined by imbedding copper constantan thermocouples created from 40-gauge Teflon coated thermocouple wire. Nine

thermocouples were inserted at the locations shown in Figure 1 and bonded to the foam

with the same graphitic bonding material as the carbon-carbon plates. Due to

temperature limitations of the thermocouple wire, the cure cycle of the bonding material

was reduced in temperature from 500 F to 300 F.
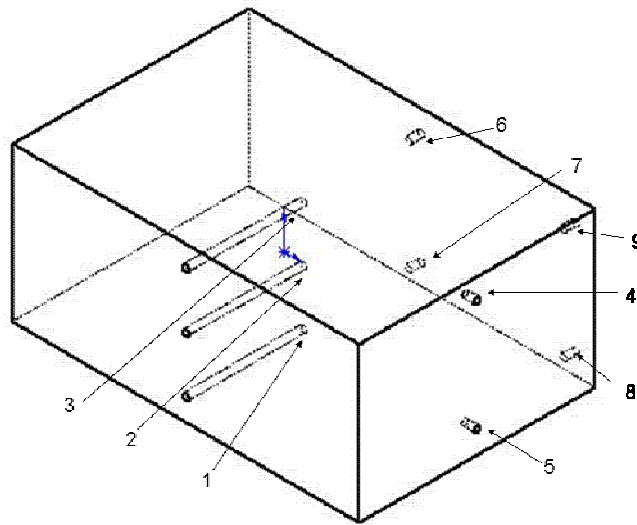
Figure 1 Thermocouple layout

For this study two phase-change materials were chosen. The first criteria used

for there selection was melting point. For the relevance to modern electronics a melting

point range of 50-100° C was chosen. Commercial grade paraffin was chosen as one of

the phase-materials because of its commonality and its melting point of 54° C. The

second phase change material chosen for this study was acetamide. Acetamide has a

melting point of 81° C allowing the study to look at another temperature point with in the

chosen range. Acetamide was also chosen for its high latent heat of 241 J/g.

Phase-change material infiltration was performed by placing the foam part at the bottom of a pool of liquefied phase-change material in a beaker. The beaker was then placed in a vacuum oven and air was removed from the interior of the oven creating a vacuum inside the oven, removing the air from the pores of the foam. Once all the air was removed from the foam part, indicated by the foam part no longer bubbling, the vacuum was released allowing the liquefied phase-change material to be forced into the foam part by atmospheric pressure. The foam part was then allowed to cool to room temperature and removed from the beaker. Excess phase change material was removed by carefully scraping with a razor blade. In order to determine the quality of the infiltration, samples were photographed by a chromo tomography (CT) scanner. The test samples were too large to fit in the scanner; therefore, their infiltration was judged by comparison of the percent by volume infiltration to smaller samples that could fit in the scanner. In Figure 2 the infiltration can be seen in a CT scan image. Dark spots in the center of the foam are voids not filled by the phase-change material. Carbon-carbon plates can be seen as solid lines on the top and bottom of the image.
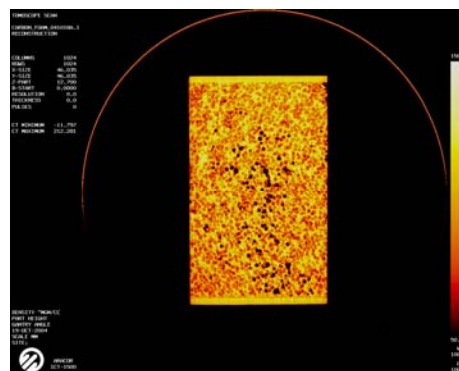

Figure 2 CT scan of phase-change material infiltration

The four open sides of the cube were sealed with 828 Epoxy Resin. This was done by placing the test article into the liquid resin and allowing the resin to cure under vacuum. By curing under vacuum, the air in the foam where phase-change material could not infiltrate was removed, leaving voids in the cured test article. These voids are a necessary part of the sample as they allow the phase-change material expansion room. The resin was then sanded down to expose the carbon-carbon plates on the top and bottom of the part for good contact with the hot and cold plates of the experiment.

Experimental Setup

The experimental setup, seen in Figure 3, was designed to provide a transient one-dimensional heat flow through the experimental sample. The setup consisted of an oxygen-free copper heat-focusing block with eleven one-kilowatt heater cartridges placed inside. This copper block was instrumented with thermocouples to measure the power flowing out of the copper block into the foam test sample.
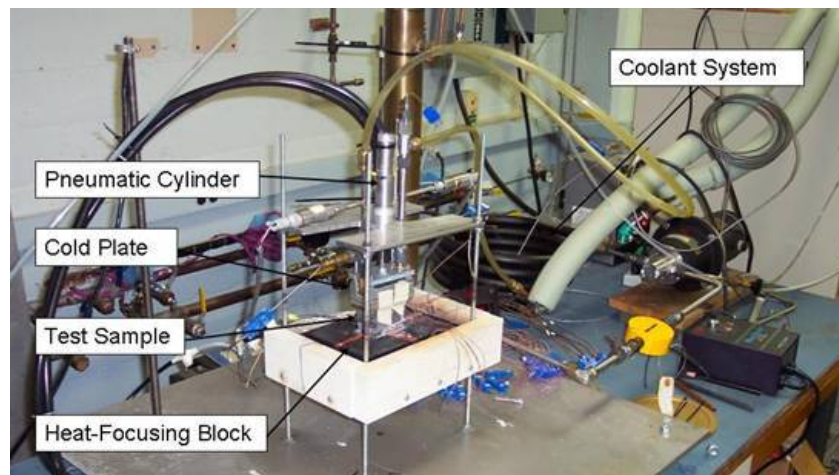
Figure 3 Experimental setup picture

A non-linear feedback control system was constructed to maintain the copper block at a constant temperature. This controller has two modes. First, the heat up mode heated the block to within 5° C of the desired temperature using 500 W of power. Once the copper was within 5° C, the control system shifted modes to the temperature maintenance mode. This mode added a flexible amount of power that varied based on the power going into the foam and the temperature of the copper block. The data acquisition unit limited the performance of this controller as the data acquisition unit only sampled once every 4 seconds. This performance limitation allowed the copper to drop 2-4 degrees Celsius upon initial application of the foam sample before the controller reacted, raising the temperature back to the desired temperature.

The foam sample was attached to a cold plate for final heat removal. The temperature of the cold plate was maintained by a flow of polyalphaolefin, PAO, a high thermal conductivity coolant used in aircraft. This cold plate provided a constant temperature boundary on the upper side of the foam sample. The cold plate and foam assembly was mounted to a pneumatic cylinder, which placed and removed the foam sample on the heat focusing plate. The pneumatic cylinder allowed this placement to happen repeatedly. It also held the sample with consistent pressure on the heat-focusing block. A flexible attachment of the pneumatic cylinder automatically adjusted for the sample being slightly out of square, producing a solid, even contact with the heat focusing block, foam sample, and cold plate.

This entire setup was designed to apply a step temperature input to the foam

sample. By applying a step temperature input, the transient temperature profile was

monitored, and the system's time constant and phase change duration were calculated.

The experiment was performed multiple times. Each time the experiment was run

something was changed. Using the different brands of foam allows the study to consider

different densities of the foam. The phase-change material was changed by using,

commercial grade paraffin, acetamide, or no phase-change material at all. The boundary

conditions were varied in accordance with the melting point of the phase-change

material, but also changed by insulating the sample from the cold plate or bringing it in

direct contact with the cold plate. In all, these different combinations created 16 different

test combinations, which are listed in Table 1.

Table 1 Experimental scenarios

Foam Type	Boundary conditions	Infiltrated medium	Boundary Temperature (C)
MER	insulated	empty	70
MER	insulated	empty	95
MER	insulated	acetamide	95
MER	insulated	paraffin	70
MER	cooled	empty	95
MER	cooled	empty	135
MER	cooled	acetamide	135
MER	cooled	paraffin	95
POCO	insulated	empty	70
POCO	insulated	empty	95
POCO	insulated	acetamide	95
POCO	insulated	paraffin	70
POCO	cooled	empty	95
POCO	cooled	empty	135
POCO	cooled	acetamide	135
POCO	cooled	paraffin	95

Theory

In order to predict the transient response, the energy balance must be considered, but this depends on the boundary conditions. The experiment looked at two categories of boundary conditions, the fully insulated and the cooled cases. In the fully insulated case, the part was insulated on all sides except where it came into contact with the copper heat-focusing block. The cooled scenario consisted of the part in contact with the copper heat-focusing block on the bottom side and in contact with the cold plate on the top and insulated on the other four sides with fiberglass insulation.

For this study, T_H, was measured just inside the copper heat-focusing block. The temperature of the foam, T_f, was measured at nine different places in the foam. For theoretical prediction the temperature was assumed to be uniform across the foam, and T_C is measured in the PAO coolant.

There are three distinct portions of the temperature curve, which must be solved for separately, first, the initial rise before the part has reached the phase-change materials melting point, second, the plateau where the phase-change material melts, and third, the final rise where the phase change has occurred and the part is increasing in temperature again. These portions were predicted by solving for the time constant of the portion of the curve when the phase-change material is solid and liquid, solving for the duration of the phase-change, and finally assembling the three curves.

In order to determine the response of the foam, first begin by attempting to determine the thermal resistance from the boundary conditions to the foam sample. This

was accomplished be setting up a thermal resistance network and solving for the total resistance. This was done on the hot side and the cold side of the foam sample.

On the hot side the heat must flow through a section of copper, a contact joint with a phase-change thermal grease, the carbon-carbon plates, a layer of bonding material, and finally a short distance into the foam. In a resistance network the joint looks like Figure 4.

T Hot ⟶ ⋀⋀⋀ ⋀⋀⋀ ⋀⋀⋀ ⋀⋀⋀ ⋀⋀⋀ ⟶ T Foam

R copper   R Phase Change Grease   R C-C plate   R Bonding Material   R foam
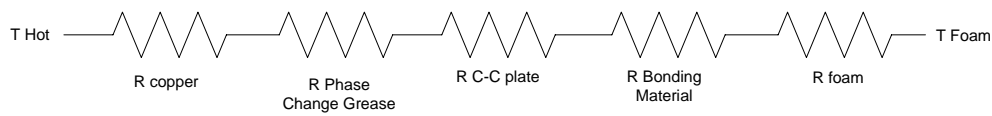
Figure 4 Thermal resistance network (hot side)

The copper resistance, the carbon-carbon plate resistance, the bonding material resistance, and the foam resistance are calculated from equation 1.

$$R = \frac{L}{k \cdot A}$$ **(1)**

Where R is the thermal resistance, L is the length the heat must flow through, k is the thermal conductivity of the material, and A is the cross-sectional area of the material. The resistance of the phase-change grease is given in manufacturer specifications. The total resistance, R_H, is calculated by summing each individual resistance.

On the cold side, the heat must flow through a section of carbon foam, the bonding material, the carbon-carbon plate, the phase-change thermal grease, a copper plate, through a offset fin heat exchanger to the PAO. This is shown in a resistance network schematic in Figure 5.

15
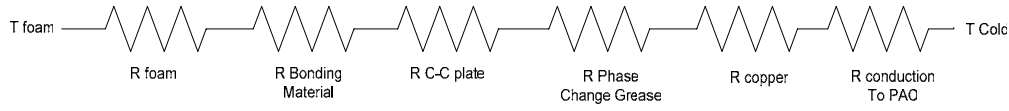
Figure 5 Thermal resistance network (cold side)

Once again the copper, carbon-carbon plate, bonding material, and the foam resistances are calculated. The resistance of the phase-change grease is taken from manufacturer specifications, and the conduction resistance to the PAO through a copper fin array is taken from Cao's *A Liquid cooler module with Carbon Foam for Cooling Applications*. The total resistance, R_C, is the summation of the separate resistances.

It must be pointed out that the above resistance calculations can only represent a lower bound estimate for the actual thermal resistance. The actual thermal resistance will include a contact resistance, between the carbon-carbon plate and the copper, most reliably determined experimentally due to the complexity of contact resistance (7:79-81). Lower bound estimates for the R_H and R_C are required for solving for the time constants. In order to determine how close the method below could get to the correct solution for the transient response a separate calculation was performed using the same method but replacing R_H and R_C with experimentally determined values.

To solve for the time constants, first, consider the case where the part is heated but is insulated from the cold plate. If we assume perfect insulation there is no heat flux out of the part ($\dot{E}_{out} = 0$). The energy rate balance ($\dot{E}_{in} - \dot{E}_{out} = \dot{E}_{stored}$) then becomes

16

$$q_{in} = (M_f \cdot c_f + M_{PCM} \cdot c_{PCM}) \cdot \frac{dT}{dt} \qquad (2)$$

q_{in} = heat flux into the foam

M_f = Mass of foam

c_f = specific heat of foam

M_{PCM} = Mass of PCM

c_{PCM} = specific heat of PCM

Substituting $q_{in} = \frac{T_H - T_f}{R_H}$ and the performing a change of variables by letting $\theta = T_f - T_H$

and noticing that $\frac{dT}{dt} = \frac{d\theta}{dt}$ (7:213) the equation becomes

$$-\frac{\theta}{R_H} = (M_f \cdot c_f + M_{PCM} \cdot c_{PCM}) \cdot \frac{d\theta}{dt} \qquad (3)$$

This equation is now a separable ordinary differential equation. In order to integrate, the variables are separated as shown in equation 4.

$$\int \frac{-1}{R_H \cdot (M_f \cdot c_f + M_{PCM} \cdot c_{PCM})} dt = \int \frac{1}{\theta} d\theta \qquad (4)$$

This integrates to

$$\frac{-t}{R_H \cdot (M_f \cdot c_f + M_{PCM} \cdot c_{PCM})} = \ln(\frac{\theta}{\theta_i}) \qquad (5)$$

Changing the variables back and simplifying, the function becomes

17

$$T_f = T_H - (T_H - T_i) \cdot e^{-\left(\frac{t}{R_H \cdot (M_f \cdot c_f + M_{PCM} \cdot c_{PCM})}\right)} \tag{6}$$

T_f=Temperature of the foam at time t

T_H = Temperature of hot boundary condition

T_i=initial temperature of the foam

R_H = Thermal resistance into the foam

From this, the time constant τ can be defined as $\tau = R_H \cdot (M_f \cdot c_f + M_{PCM} \cdot c_{PCM})$.

For the second case, where the foam block is placed against the cold plate the heat flux out is no longer zero. The energy rate balance becomes

$$q_{in} - q_{out} = (M_f \cdot c_f + M_{PCM} \cdot c_{PCM}) \cdot \frac{dT}{dt} \tag{7}$$

q_{in} remains the same and $q_{out} = \dfrac{T_f - T_c}{R_c}$ which when substituted in and simplified makes

the energy rate equation

$$\frac{R_c \cdot T_H + R_H \cdot T_c}{R_c \cdot R_H} - \frac{R_C + R_H}{R_C \cdot R_H} \cdot T_f = (M_f \cdot c_f + M_{PCM} \cdot c_{PCM}) \cdot \frac{dT}{dt} \tag{8}$$

Solving this equation is slightly more complex. It can, however, be solved by the use of integrating factors. Putting into the form $y' + Py = Q$ the standard form for integrating factors

$$\frac{dT}{dt} + \left(\frac{R_C + R_H}{R_C \cdot R_H \cdot (M_f \cdot c_f + M_{PCM} \cdot c_{PCM})}\right) \cdot T = \frac{R_C \cdot T_H + R_H \cdot T_C}{R_C \cdot R_H \cdot (M_f \cdot c_f + M_{PCM} \cdot c_{PCM})} \tag{9}$$

18

By defining $I = \int P dt$ the solution becomes $y = e^{-I} \int Q e^I dt + C e^{-I}$ (3:347). After plugging in the variables for this problem

$$T = e^{-\left(\frac{R_C + R_H}{R_C \cdot R_H \cdot (M_f \cdot c_f + M_{PCM} \cdot c_{PCM})}\right) \cdot t} \cdot \int \left(\frac{R_C \cdot T_H + R_H \cdot T_C}{R_C \cdot R_H \cdot (M_f \cdot c_f + M_{PCM} \cdot c_{PCM})}\right) \cdot e^{\left(\frac{R_C + R_H}{R_C \cdot R_H \cdot (M_f \cdot c_f + M_{PCM} \cdot c_{PCM})}\right) \cdot t}$$
$$+ C \cdot e^{-\left(\frac{R_C + R_H}{R_C \cdot R_H \cdot (M_f \cdot c_f + M_{PCM} \cdot c_{PCM})}\right) \cdot t} \tag{10}$$

Performing some reduction and solving the integration the equation for the temperature of the foam becomes

$$T = \frac{R_C \cdot T_H + R_H \cdot T_C}{R_C + R_H} + C \cdot e^{-\left(\frac{R_C + R_H}{R_C \cdot R_H \cdot (M_f \cdot c_f + M_{PCM} \cdot c_{PCM})}\right) \cdot t} \tag{11}$$

Solving for the integration constant C by letting T=T$_i$ at time t=0 the final equation for the temperature of the foam becomes

$$T = \frac{R_C \cdot T_H + R_H \cdot T_C}{R_C + R_H} + \left(T_i - \frac{R_C \cdot T_H + R_H \cdot T_C}{R_C + R_H}\right) \cdot e^{-\left(\frac{R_C + R_H}{R_C \cdot R_H \cdot (M_f \cdot c_f + M_{PCM} \cdot c_{PCM})}\right) \cdot t} \tag{12}$$

From this, the time constant τ for the cooled case can be defined as

$$\tau = \frac{R_c \cdot R_H \cdot (M_f \cdot c_f + M_{PCM} \cdot c_{PCM})}{R_c + R_H} \tag{13}$$

This is not the complete solution for the transient response because the phase-change plateau must also be solved.

Once the system reaches the melting point of the material, the system temperature will plateau for a short time while the phase change takes place. This time can be calculated by starting with an energy balance on the foam sample. By drawing a control volume just inside the foam part, the energy balance equation is:

$$E_{in} - E_{out} = E_{stored} \tag{14}$$

Letting $E_{in} = q_{in} \cdot t$, $E_{out} = \sum (q_{out} \cdot t)$, and $E_{stored} = M_{PCM} \cdot h_{sf}$, where h_{sf} is latent heat of fusion of the phase change material the energy balance becomes

$$q_{in} \cdot t - \sum (q_{out} \cdot t) = M_{PCM} \cdot h_{sf} \tag{15}$$

The time, t, can be factored out and solved, developing an equation for the time for the phase change to occur.

$$t_{pha\sec hange} = \frac{M \cdot h_{sf}}{q_{in} - \sum q_{out}} \tag{16}$$

After solving for the time constant and the duration of the phase change the predicted transient temperature profile can be assembled for each case. Using this temperature profile the power flowing into the foam can be predicted by using

$$q = \frac{T_H - T_f}{R_H} \tag{17}$$

20

IV. Results and Analysis

Bonding Results

During bonding the ultimate goal is to reduce the thermal resistance, allowing heat to flow easily. The thermal resistance is calculated by equation 1. The bonding material fixes k, and A is fixed by the geometry of the part. Therefore, in order to minimize the thermal resistance of the bond, L must be kept to a minimum. By viewing under a microscope, the bond can be seen and inspected for thickness, voids, and consistency. In Figure 6 a bond can be seen between the carbon-carbon plate, on the bottom, and the carbon foam on the top. Small voids can be seen near the edge of the part. Voids will reduce the area of the bond and, therefore, increase the thermal resistance of the bond.
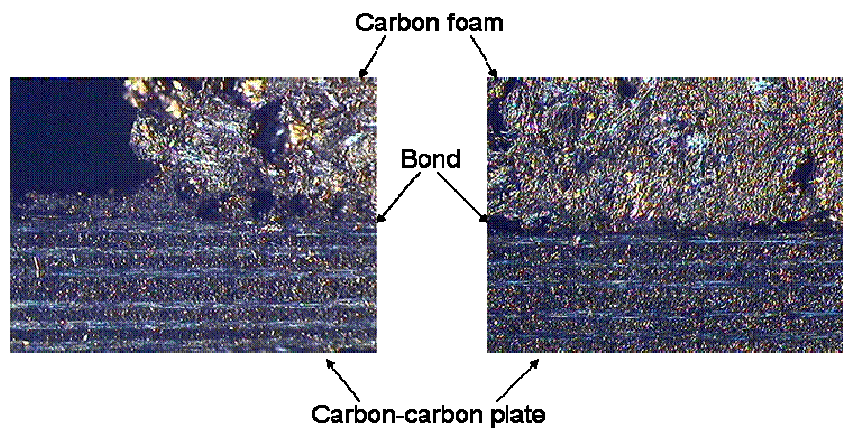
Figure 6 First bond

The bond is very thin with numerous voids. This bond is 0.013 cm thick. This attempt at bonding failed and was judged to be too thin. The second attempt at bonding can be seen in Figure 7. This bond is thicker and has fewer voids.   This bond is 0.025 cm thick and strong enough that the carbon-carbon plates fail before the bond breaks.
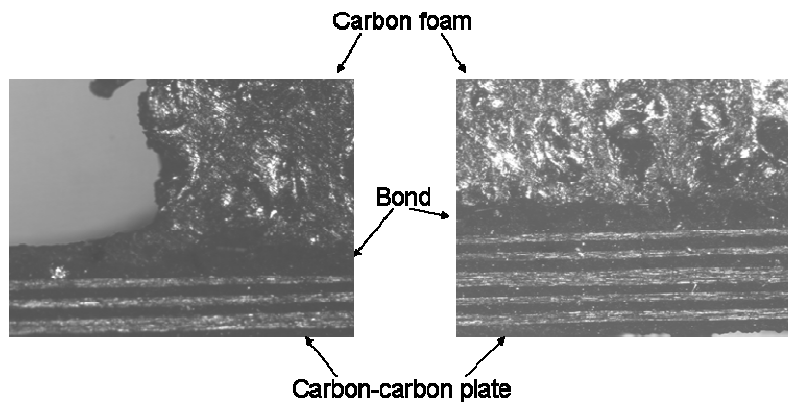
Figure 7 Second bond

Without moving to more precise and complex techniques for creating the bond the 0.025 cm thick bond is accepted to minimize the thermal resistance and still be strong enough to hold the part together for the experiment.

Infiltration Results

Chromo Tomography (CT) scans were used to judge the infiltration. CT scans allowed the infiltration to be seen without damaging the part itself. The first infiltration can be seen in Figure 8.
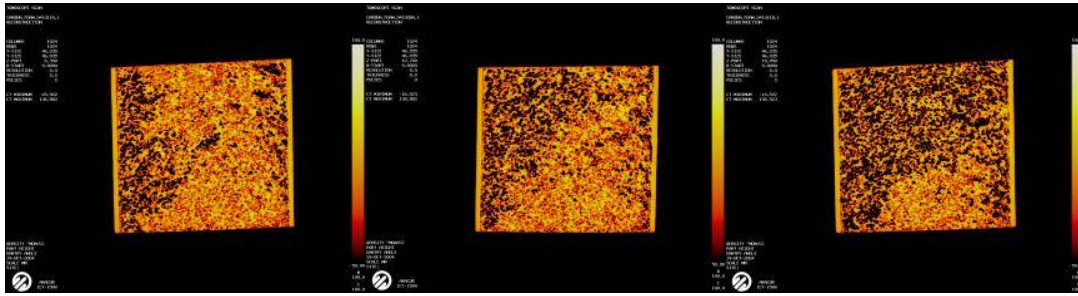
Figure 8 CT scan of first infiltration

Each image represents a *slice* at a different depth of the part. The carbon-carbon plates

can be seen on the left and right sides. The black areas are voids in the foam that were

not infiltrated with the phase-change material. This particular part had only 34% by

volume phase-change material. This percentage is calculated from the mass of the phase-

change material, the density of the phase-change material, and the dimensions of the

foam.

After modifying the infiltration technique, a second part was infiltrated and

imaged. This part can be seen in Figure 9.
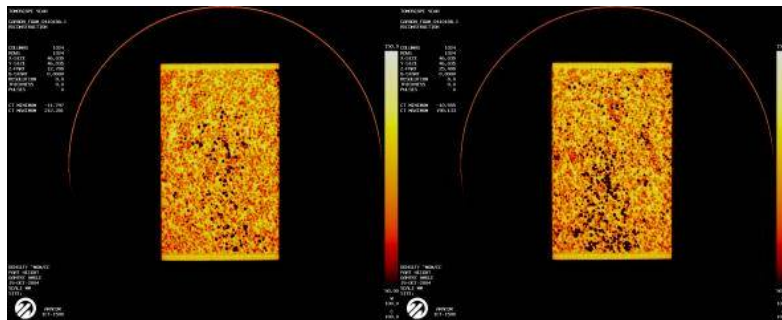
Figure 9 CT scan of second infiltration

Once again the two images are the same part imaged at different depths. Here fewer non-infiltrated voids are present. This part is 42% by volume phase change material, a complete enough infiltration to be used for the experimental parts.

The experimental parts were infiltrated using the same technique and had similar results. The experimental parts and the infiltration percentages can be seen in Table 2.

Table 2 Infiltration results

Sample	% Infiltration by Volume
A - Paraffin	48.99
B - Acetamide	54.27
C - Paraffin	44.44
D -Paraffin	48.26
M1 -Paraffin	63.70
M3 - Acetamide	63.77

Experimental Results

Each test run was performed and analyzed. The time constants were taken from the data by performing a curve fit on the center thermocouple data, thermocouple number 2, during the transient portion of the curve. This transient portion was considered the portion where the temperature of the part was less than 99% of the final temperature in the empty sample scenarios. When phase change material was in the part the time constant was determined from only the data less than 10 degrees below than the phase change temperature. By only using this portion of the curve the curve fit is able to be performed without incorporating the effects of the phase change. This was performed using the equation 18.

24

$$T(t) = T_{ss} - (T_{ss} - T_i) \cdot e^{-t/\tau}$$

(18)

Where T_{ss} is the maximum temperature the part reaches during the test and T_i is the

temperature the foam part before heat is added. Since t is known for each data point τ

can be calculated for each data point. The time constants for all the data points in the

transient region of the curve are averaged to solve for one time constant for the entire

curve. τ was then plugged back into equation 18 and plotted.   The experimental scenario

with MER foam, no phase change material, no cooling, and a boundary condition of 70 C

is shown in Figure 10.

Time Constant (MER, Empty, Insulated, 70C)
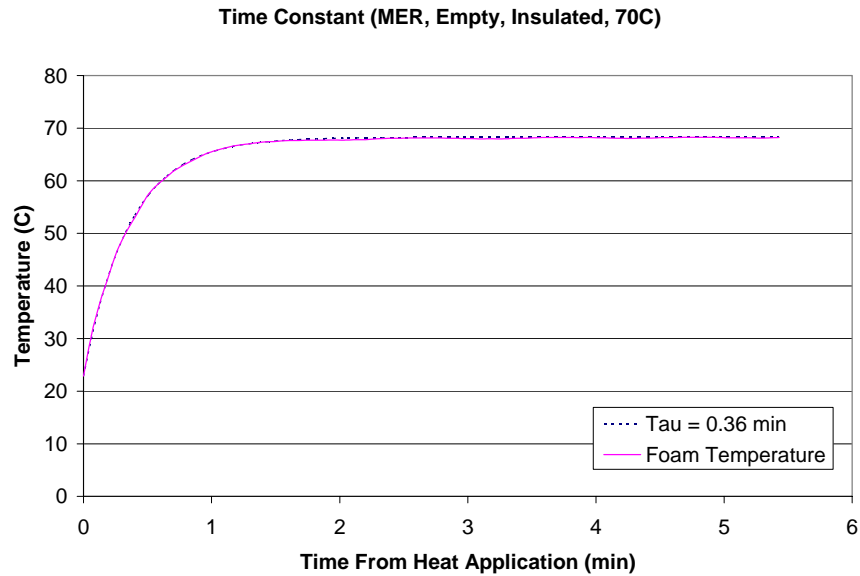
Figure 10 Time constant curve fit

This process is repeated for each experimental scenario. The plots for all the

other experimental scenarios are in Appendix C. The time constants for each

experimental scenario are in Table 3.

25

Predicted time constants were consistently faster than the curve fit time constants.

This comparison is shown in Table 4. This difference is expected to come from two

sources. First, the contact resistances predicted were a lower bound estimate only. If

these values were increased, the predicted time constant would be slower. This

hypothesis was tested by calculating a predicted time constant using the method

described in the Theory section but replacing the resistance calculated using the

resistance network, with experimentally determined contact resistances.

Table 3 Time constant experimental results

Foam Type	Boundary Conditions	Infiltrated Medium	Boundary Temperature (C)	Curve Fit Time Constant (min)
MER	insulated	empty	70	0.36
MER	insulated	empty	95	0.40
MER	insulated	acetamide	95	0.80
MER	insulated	paraffin	70	0.68
MER	cooled	empty	95	0.27
MER	cooled	empty	135	0.27
MER	cooled	acetamide	135	1.07
MER	cooled	paraffin	95	0.96
POCO	insulated	empty	70	0.47
POCO	insulated	empty	95	0.51
POCO	insulated	acetamide	95	1.30
POCO	insulated	paraffin	70	0.95
POCO	cooled	empty	95	0.40
POCO	cooled	empty	135	0.42
POCO	cooled	acetamide	135	0.56
POCO	cooled	paraffin	95	0.64

These experimental contact resistances were calculated from the experimental

data at each point by utilizing equation 19 and 20.

$$R_H = \frac{T_{copper} - T_{foam}}{q_{in}} \tag{19}$$

$$R_C = \frac{T_{foam} - T_{PAO}}{q_{out}}$$ **(20)**

The resistances calculated at all data points were averaged to determine experimental

resistance for each scenario.   Table 4 shows that the time constants calculated using the

experimentally determined contact resistances produces a more accurate solution.

Other sources of error come from simplifications made during the analytic

analysis. The analytic analysis left out heat losses to the sides of the foam part. The

predicted time constant would be closer to the experimental values if those losses had

been included and the differential equation still solvable.

Table 4 Predicted vs. experimental time constants

Foam Type	Boundary Conditions	Infiltrated Medium	Boundary Temperature (C)	Curve Fit Time Constant (min)	Predicted Time Constant Theoretical (min)	Percent Different (%)	Predicted Time Constant Experimental R (min)	Percent Different (%)
MER	insulated	empty	70	0.36	0.21	41%	0.20	45%
MER	insulated	empty	95	0.40	0.21	47%	0.23	41%
MER	insulated	acetamide	95	0.80	0.64	20%	0.55	32%
MER	insulated	paraffin	70	0.68	0.69	1%	0.51	25%
MER	cooled	empty	95	0.27	0.17	37%	0.26	3%
MER	cooled	empty	135	0.27	0.17	37%	0.26	2%
MER	cooled	acetamide	135	1.07	0.51	52%	1.14	7%
MER	cooled	paraffin	95	0.96	0.55	43%	0.81	16%
POCO	insulated	empty	70	0.47	0.32	31%	0.48	3%
POCO	insulated	empty	95	0.51	0.32	36%	0.32	37%
POCO	insulated	acetamide	95	1.30	0.71	45%	0.75	42%
POCO	insulated	paraffin	70	0.95	0.70	27%	0.76	20%
POCO	cooled	empty	95	0.40	0.26	36%	0.31	21%
POCO	cooled	empty	135	0.42	0.26	39%	0.40	5%
POCO	cooled	acetamide	135	0.56	0.56	1%	1.15	106%
POCO	cooled	paraffin	95	0.64	0.55	14%	0.47	27%
					Average	32%		27%

The time the part took to undergo the phase change was also taken from the raw

data. The phase change time was obtained from the experimental data by shifting the

exponential curve until it lined up with the curve after the phase change. An example can be seen in Figure 11. All the other cases are plotted in Appendix C.

Time Constant (Poco, Acetamide, Insulated, 95C)
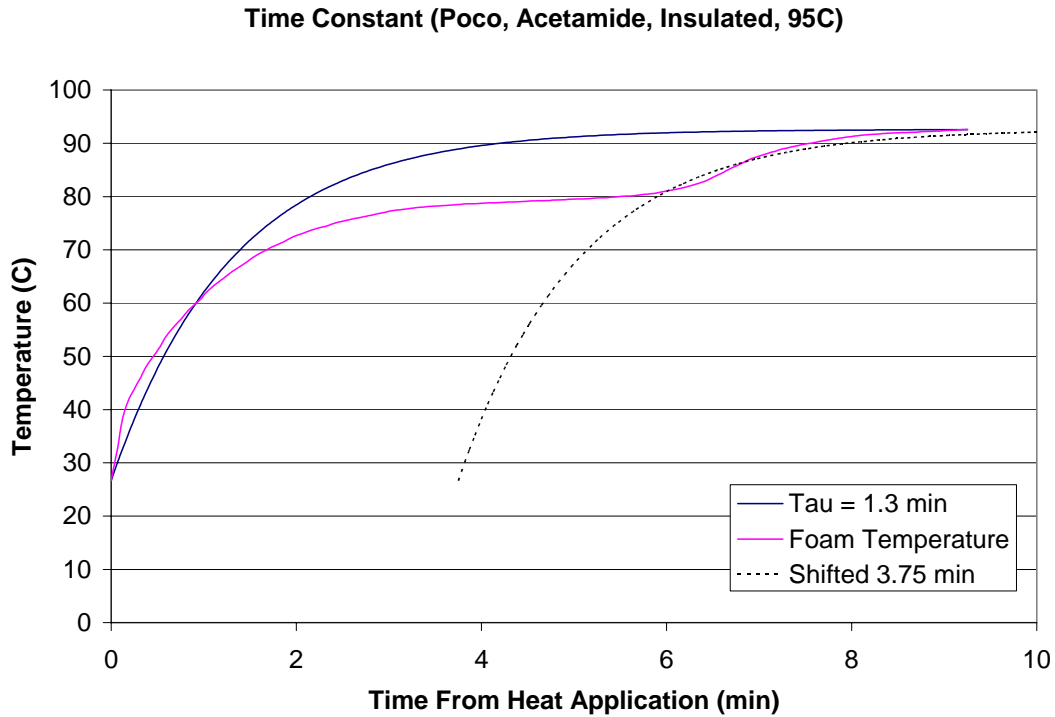
Figure 11 Phase change time determination method

This process creates a consistent method of reading the phase change time from the experimental data for each case. The phase change times are listed in Table 5.

The prediction of the phase change time was consistently shorter than the experimental results as shown in Table 6. Once again the thermal resistances calculated from the contact resistances were the source of some of the error. The phase change times were re-calculated using the experimentally determined contact resistance to show the effect of knowing the actual contact resistance. This comparison is shown in Table 6.

Table 5 Phase change time experimental results

Foam Type	Boundary Conditions	Infiltrated Medium	Boundary Temperature (C)	Actual Phase Change Time (min)
MER	insulated	acetamide	95	5.0
MER	insulated	paraffin	70	2.0
MER	cooled	acetamide	135	5.0
MER	cooled	paraffin	95	1.6
POCO	insulated	acetamide	95	3.8
POCO	insulated	paraffin	70	2.5
POCO	cooled	acetamide	135	3.1
POCO	cooled	paraffin	95	1.1

Even when the contact resistance is known there was still variation between the calculated phase change time and the actual phase change time. This variation could come from the assumption that the sample was a uniform block of phase-change material, when in fact the sample was a composite of foam and phase-change material. This composite has void spaces that prevent the heat from easily flowing into the phase-change material from the foam. It is also possible that the phase-change material shrunk in the process of freezing, leaving a poor contact between the foam and the phase-change material which would inhibit the heat flow into the phase-change material, causing the phase change to take longer than the simple case calculated.

There is a second possible reason for the difference in the predicted phase-change time and the actual phase-change time. The plateau was not at constant temperature. The sample is increasing in temperature during the phase-change. This increase in temperature pulls heat energy away from the phase change causing the phase-change to take longer than predicted by changing the energy balance from

$$q_{in} \cdot t - \sum (q_{out} \cdot t) = M_{PCM} \cdot h_{sf} \tag{21}$$

to

$$q_{in} \cdot t - \sum (q_{out} \cdot t) = M_{PCM} \cdot h_{sf} + (M_f \cdot c_f + M_{PCM} \cdot c_{PCM}) \cdot \frac{dT}{dt} \qquad (22)$$

The predicted and experimentally determined phase change times are listed in Table 6.

Table 6 Predicted vs. actual phase change time

Foam Type	Boundary Conditions	Infiltrated Medium	Boundary Temperature (C)	Actual Phase Change Time (min)	Predicted Phase Change Time (min)	Percent Different	Predicted Time For Phase Change Experimental R (min)	Percent Different
MER	insulated	acetamide	95	5.0	4.1	18%	3.5	30%
MER	insulated	paraffin	70	2.0	1.6	20%	1.2	42%
MER	cooled	acetamide	135	5.0	1.4	73%	3.1	39%
MER	cooled	paraffin	95	1.6	0.7	54%	1.3	20%
POCO	insulated	acetamide	95	3.8	3.5	6%	3.8	1%
POCO	insulated	paraffin	70	2.5	1.2	51%	1.3	46%
POCO	cooled	acetamide	135	3.1	1.2	63%	2.5	20%
POCO	cooled	paraffin	95	1.1	0.6	48%	0.6	48%
					Average	42%	Average	27%

Even though the time constants and the phase change times show the accuracy of the prediction it does not always clarify the complete solution. In order to show the complete solution the transient temperature profile prediction was laid on top of the experimental results for each case. A representative version of this comparison is shown in Figure 12 for the experimental case of Poco foam infiltrated with acetamide, placed in contact with the cold plate, and with a boundary temperature of 135° C. The measurements from three thermocouples have been plotted against the theoretical prediction. The fifth curve plotted, Experimental R, is the temperature curve calculated using the theoretical method derived above replacing the resistance network with experimentally determined contact resistances. The Experimental R curve is closer to the actual foam temperature curve reinforcing the importance of knowing accurately the contact resistance. The plots for all the experimental cases are shown in Appendix A.

Predicted vs. Actual Temperature (Poco, Acetamide, Cooled, 135C)
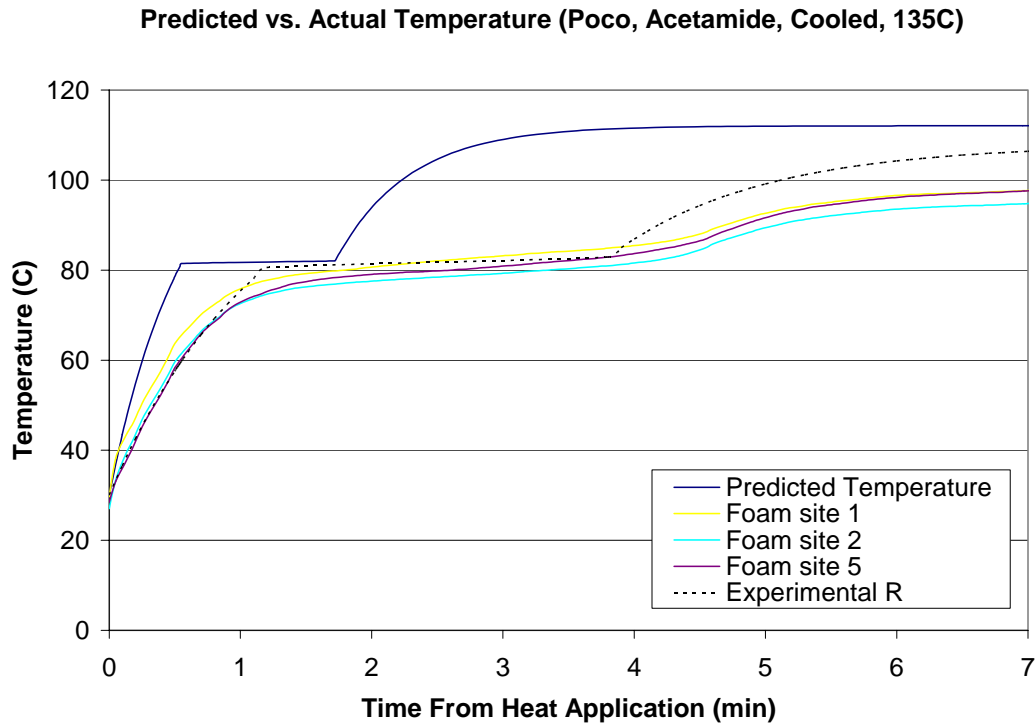
Figure 12 Predicted vs actual temperature profile

The final parameter predicted in the Theory section was the power into the foam. This predicted power into the foam was plotted against the power into the foam determined from the experiment. This comparison is shown in Figure 13 for the experimental scenario where Poco foam was infiltrated with acetamide placed in contact with the cold plate and the heat-focusing block was maintained at 135° C.   A third curve, Experimental R, is plotted using the actual contact resistance rather than the resistance calculated from the resistance network. This plot the shows the analytic method can approximate the actual power into the foam if the contact resistance is known accurately. Each experimental scenario was plotted and is shown in Appendix B.

Predicted vs. Actual Power into Foam (Poco, Acetamide, Cooled, 135C)
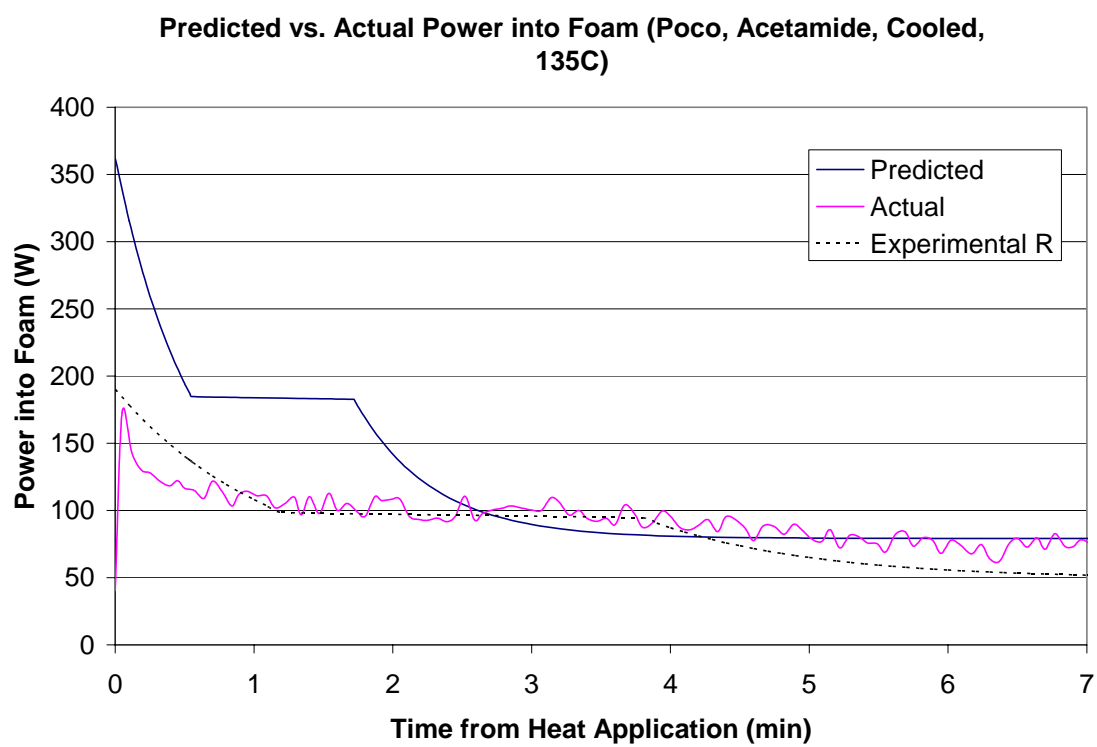
Figure 13 Predicted vs. actual power

V. Conclusion

The transient response of the foam and phase-change material was investigated by application of a step temperature heat load. The experimental response was an approximate first order exponential curve with a plateau during the phase change. A simple analytic prediction of this response was developed, and while not exact, it does provide a rough estimate of the response. This prediction would be useful for engineers considering the use of this type of system. The experimentally determined contact resistance was plugged into the theoretical prediction to show that more accuracy can be gained in the prediction if the contact resistance is known.

This study also considered the bonding of a carbon-carbon plate to carbon foam. It was found that a bond could be created consistently 0.025 cm thick with a graphitic bonding material through the use of basic techniques and a heated cure cycle.

Infiltration of the carbon foam with multiple phase-change materials was investigated. It was found that the highest infiltrations rates were achieved by placing the foam in a pool of liquefied phase-change material, pulling a vacuum on the foam and phase-change material, and releasing the vacuum once the foam had finished releasing air but while the phase change material was still liquefied. This allowed the atmospheric pressure to force the phase change material into the pores of the foam.

Recommendations for Further Study

Even though this experiment shows a response similar to what is expected, this study is limited by boundary conditions. Altering the boundary conditions will change the response of the system. Therefore, it is recommended for further study the following areas

1. Create an experiment where the boundary condition is a constant heat flux rather than a constant temperature. This would more accurately simulate an actual system, because most electronic components have a heat flux output and not a constant temperature output. By knowing the response to a constant heat flux the user of the system could predict the maximum temperature reached for a given heat flux and the time the phase change material would prevent the system from reaching that maximum temperature. Accomplishing this would require a more complex feedback controller with a faster response and a smaller copper heat-focusing block that will respond faster to control inputs.

2. Look more in-depth at the theory of the phase-change to produce a more accurate model. By including the free convection movement of the phase change material and the interface conditions with the foam, a more complex and more accurate model could be developed to predict the response.

3. Expand the study to include more phase change materials and more variations in the foam properties.

4. Look at the cooling response. An investigation into the cooling response of the foam and phase-change material would allow the prediction of the response of a system with an oscillatory heat loading profile.

Appendix A: Time vs. Temperature Plots

Predicted vs. Actual Temperature (MER, Empty, Insulated, 70C)
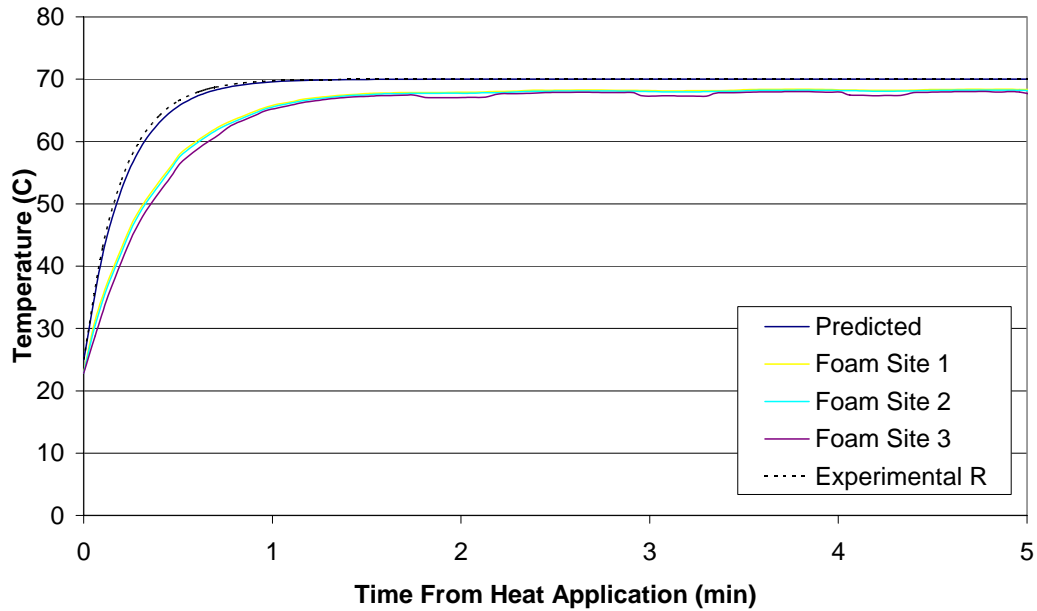
Predicted vs. Actual Temperature (MER, Empty, Insulated, 95C)

36
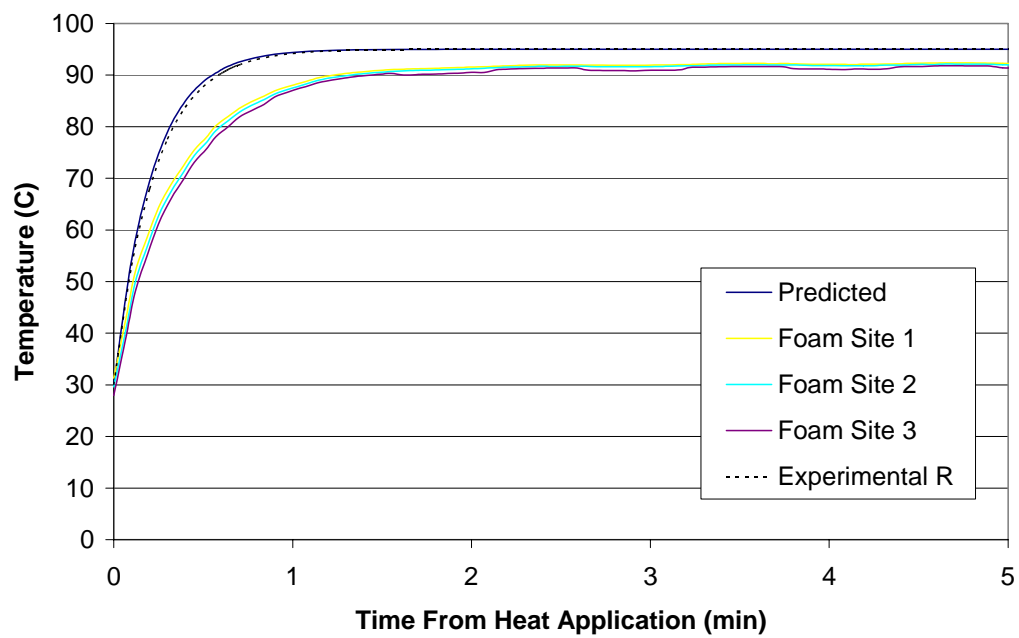
Predicted vs. Actual Temperature (MER, Acetamide, Insulated, 95C)
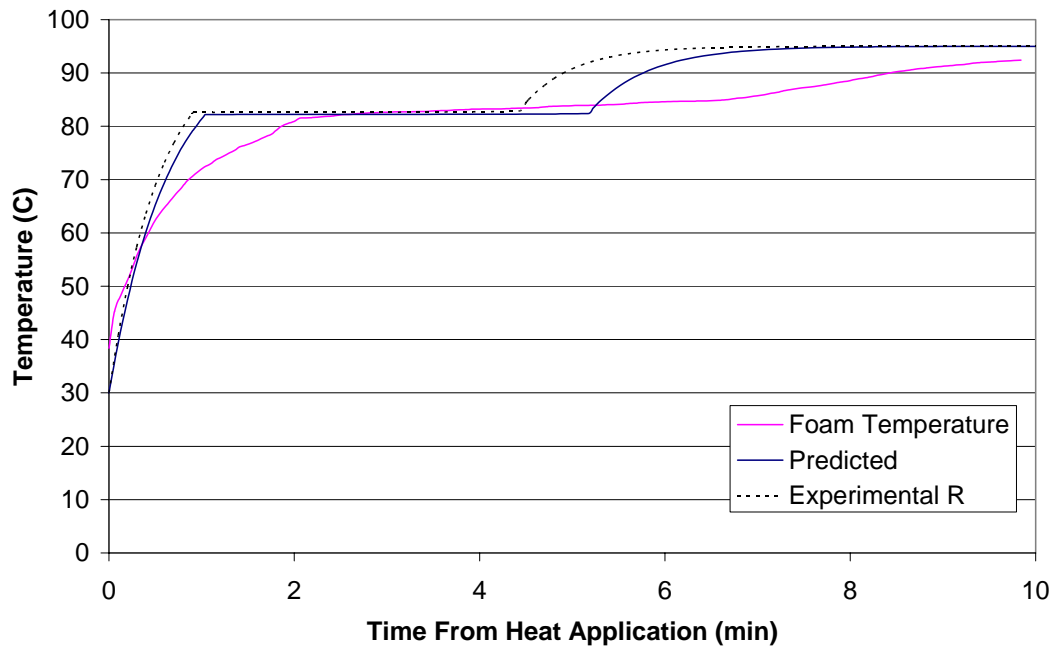
Predicted vs. Actual Temperature (MER, Paraffin, Insulated, 70C)
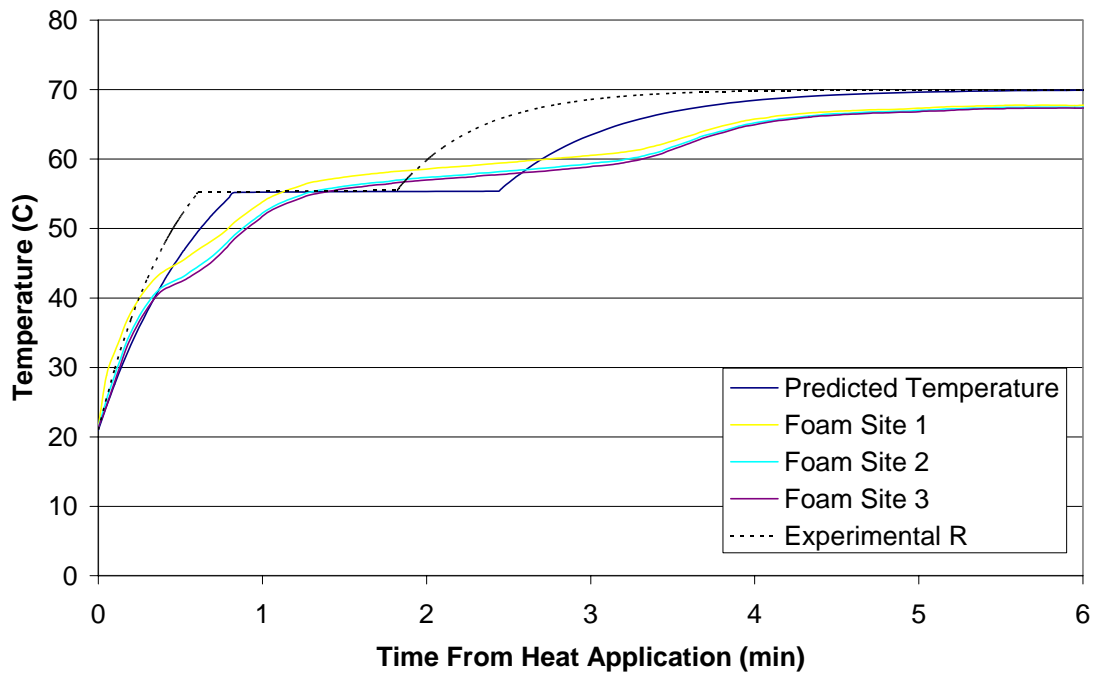
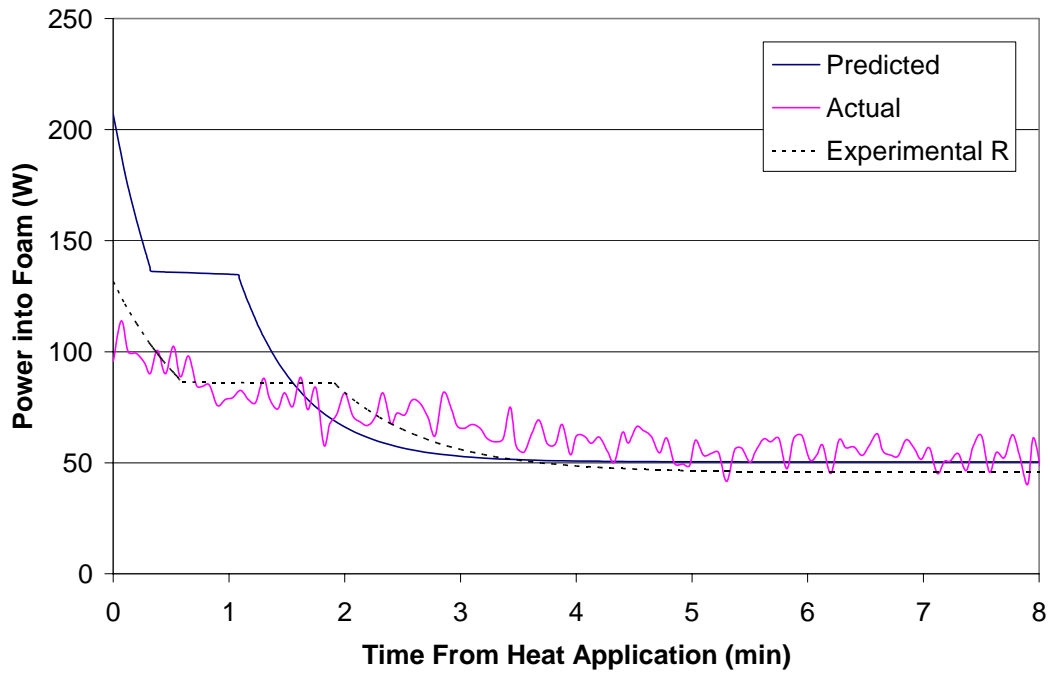**Predicted vs. Actual Temperature (MER, Empty, Cooled, 95C)**
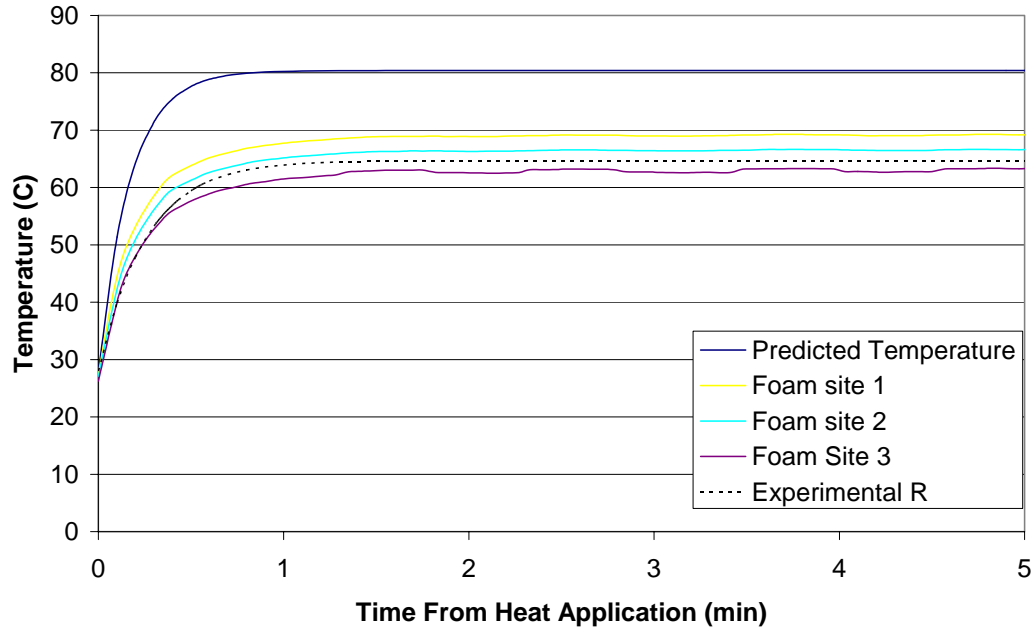
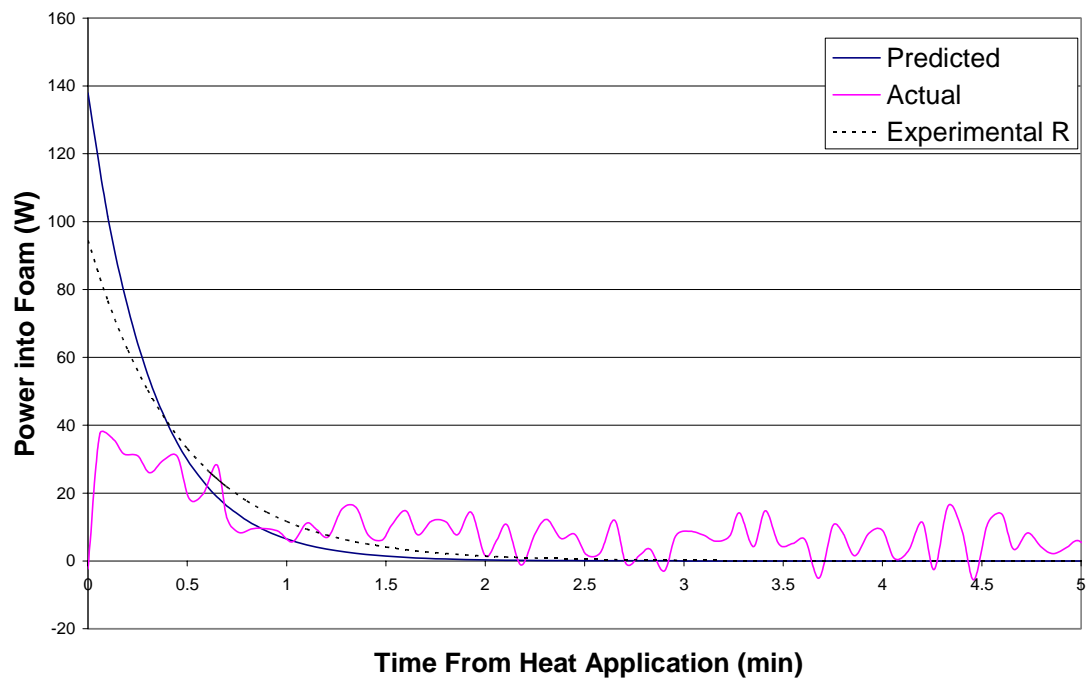**Predicted vs. Actual Temperature (MER, Empty, Cooled, 135C)**
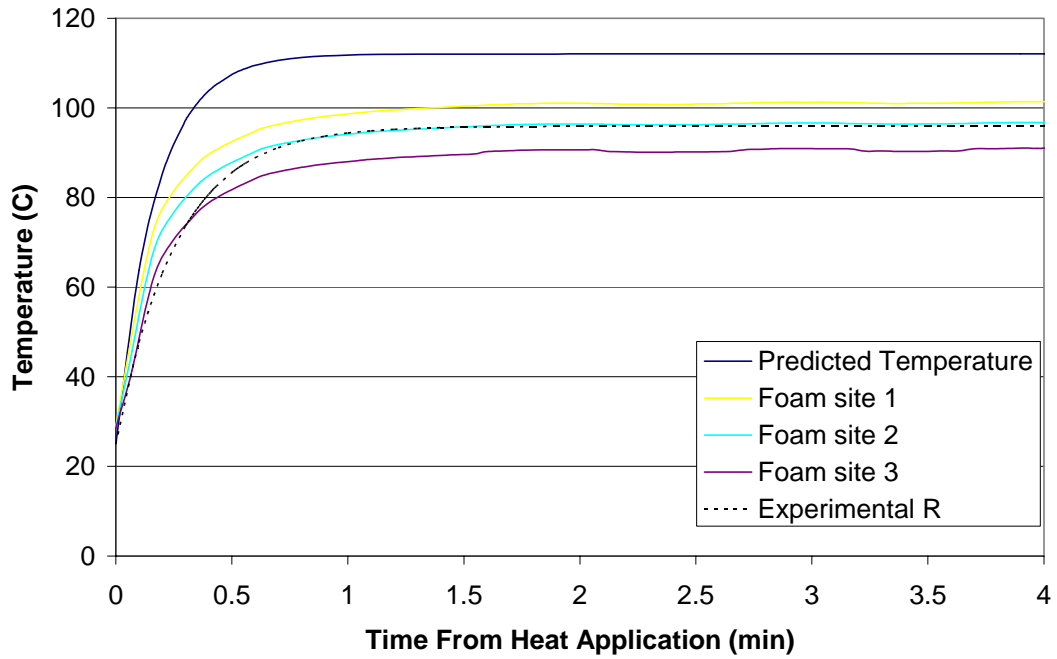
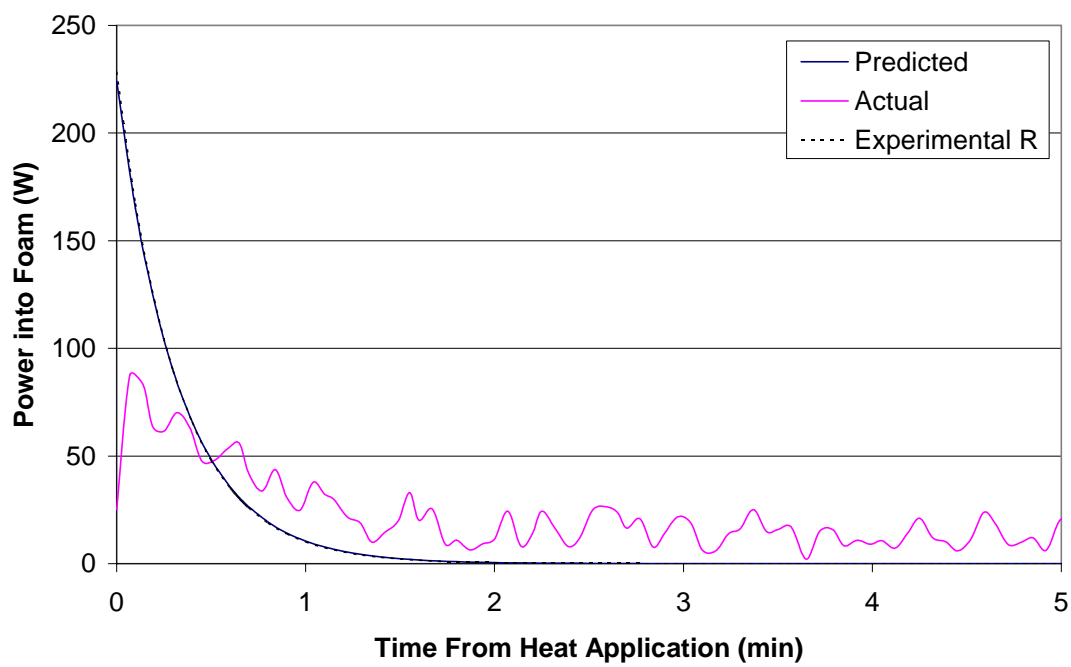**Predicted vs. Actual Temperature (MER, Acetamide, Cooled, 135C)**
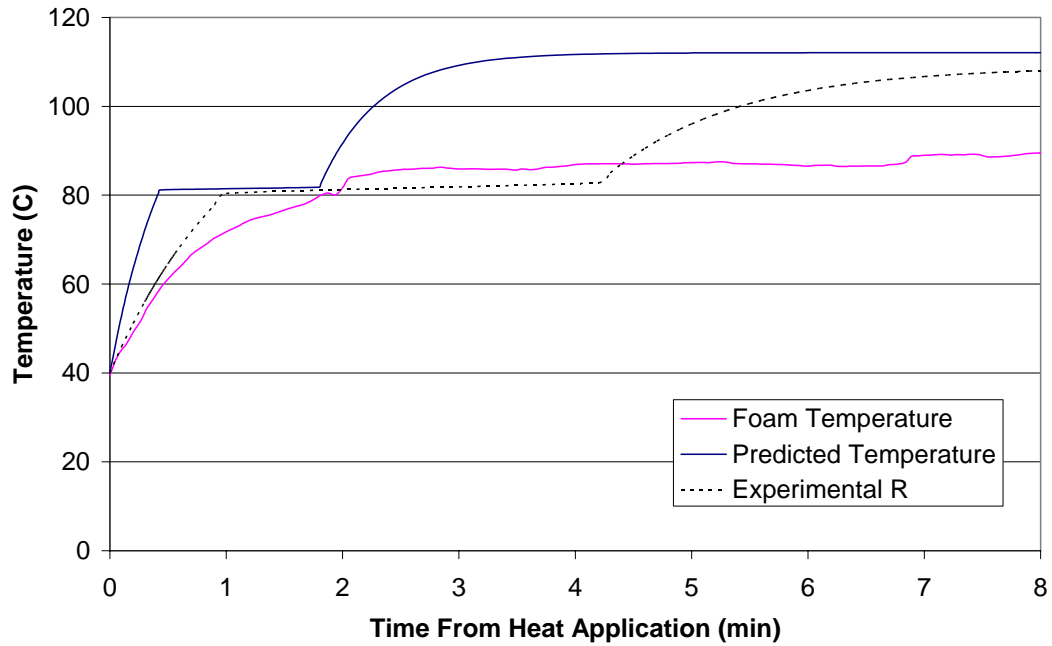
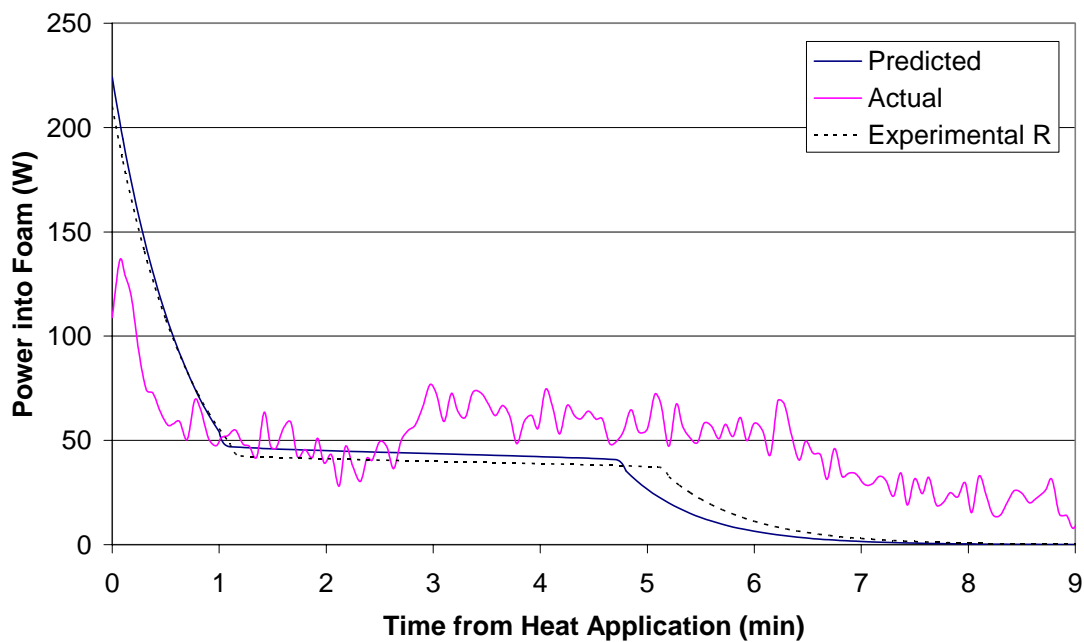**Predicted vs. Actual Temperature (MER, Paraffin, Cooled, 95C)**
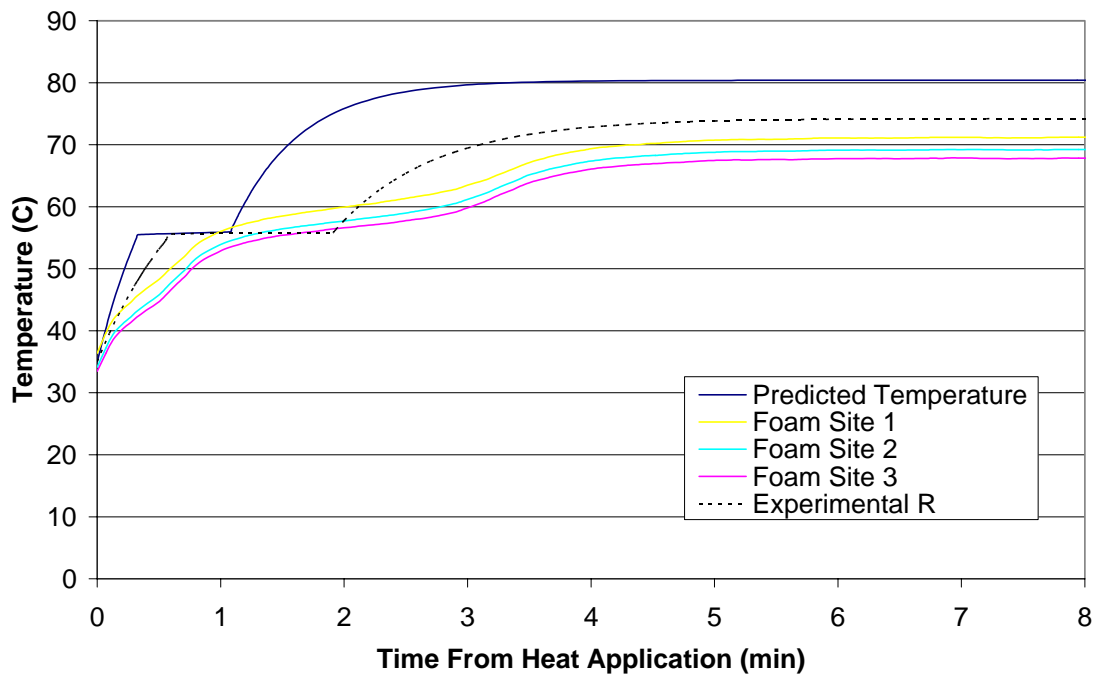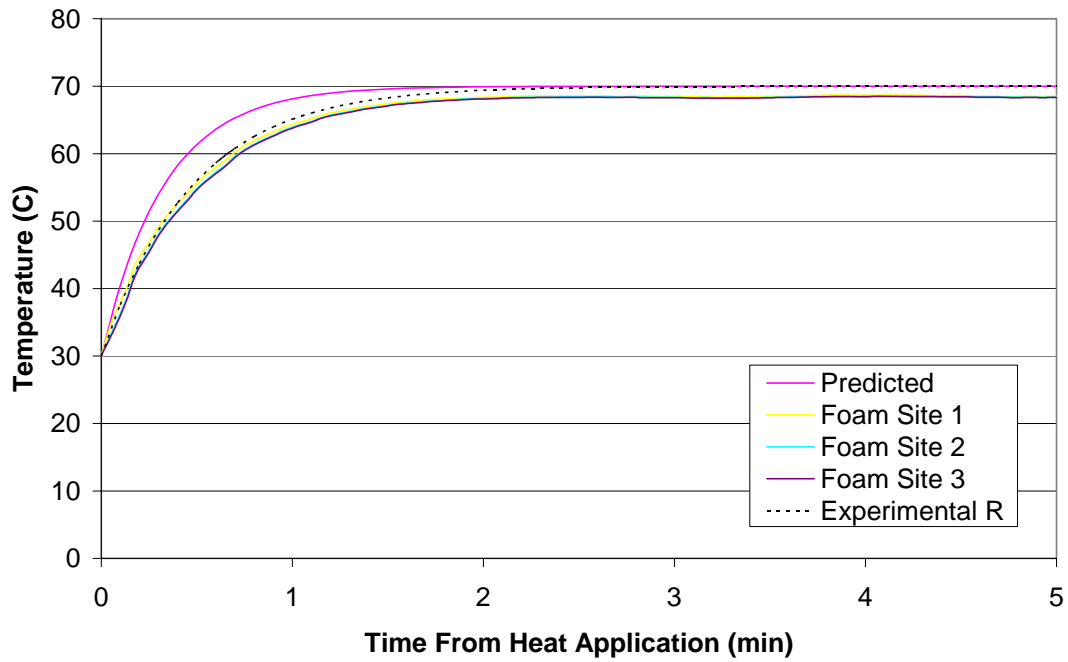
Predicted vs. Actual Temperature (Poco, Empty, Insulated, 70C)

Predicted vs. Actual Temperature (Poco, Empty, Insulated, 95C)
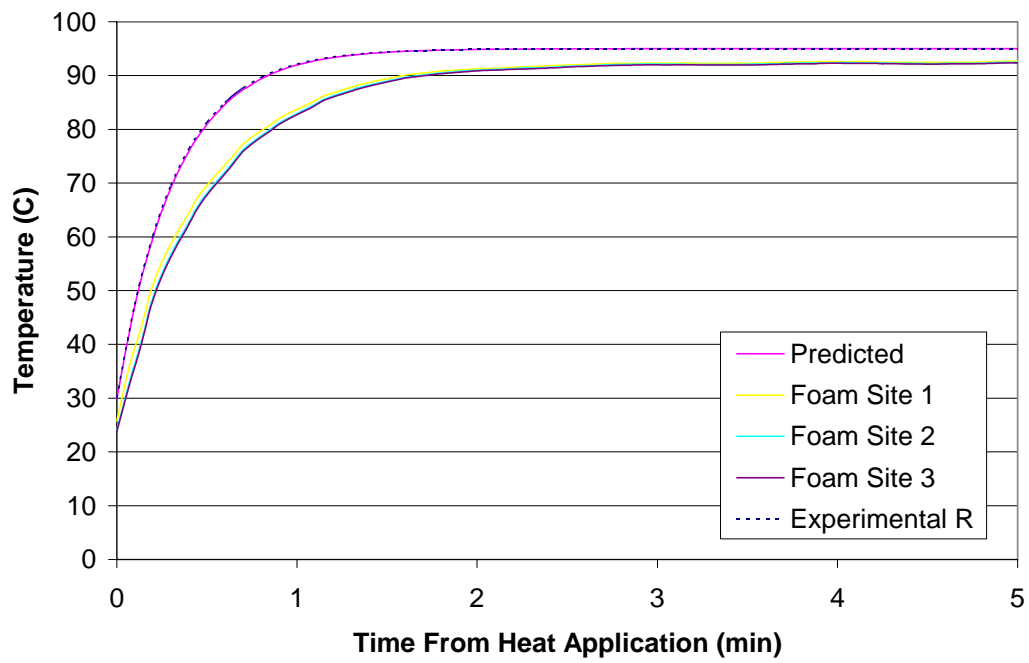
Predicted vs. Actual Temperature (Poco, Acetamide, Insulated, 95C)
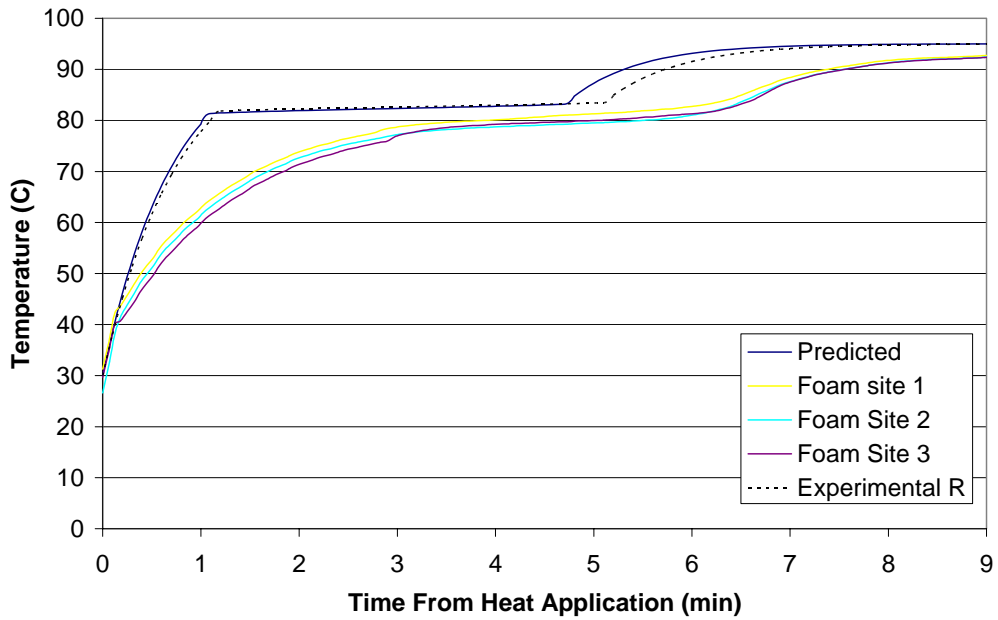
Predicted vs. Actual Temperature (Poco, Paraffin, Insulated, 70C)
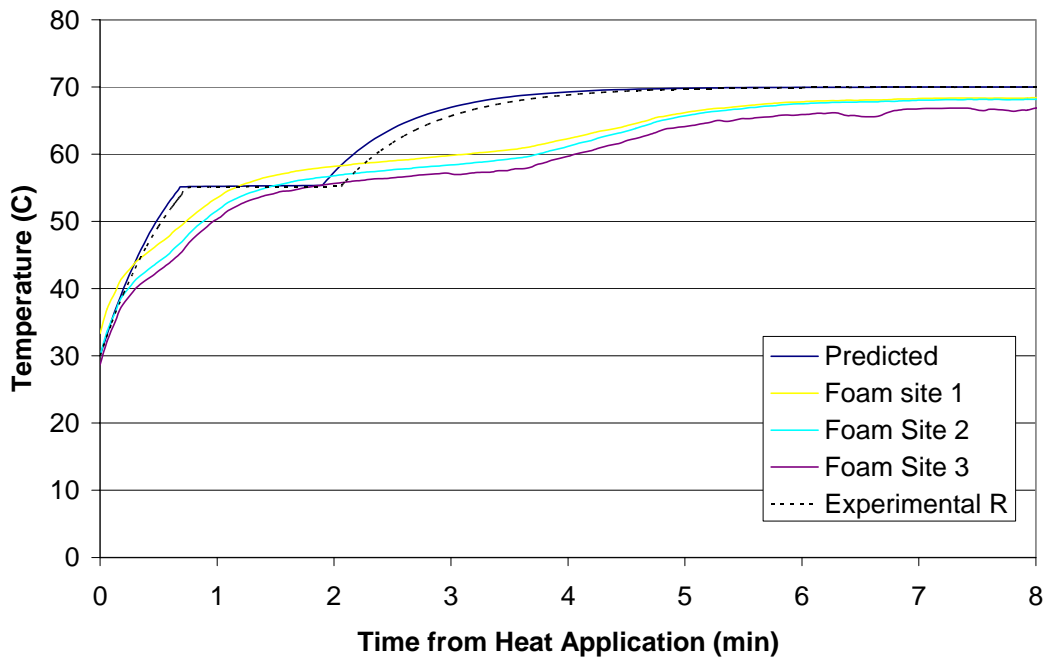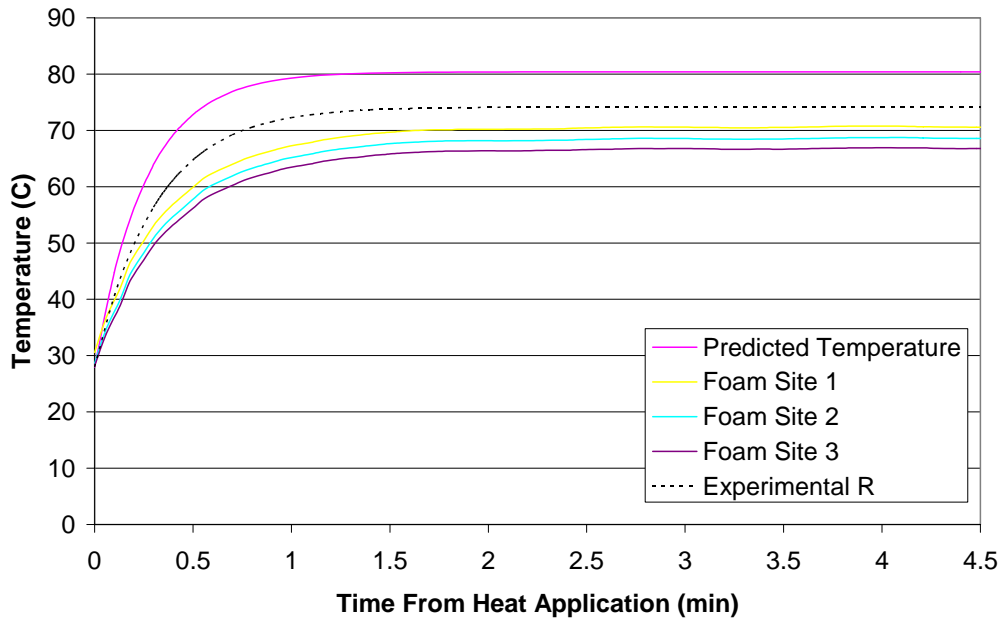
Predicted vs. Actual Temperature (Poco, Empty, Cooled, 95C)

Predicted vs. Actual Temperature (Poco, Empty, Cooled, 135C)

42
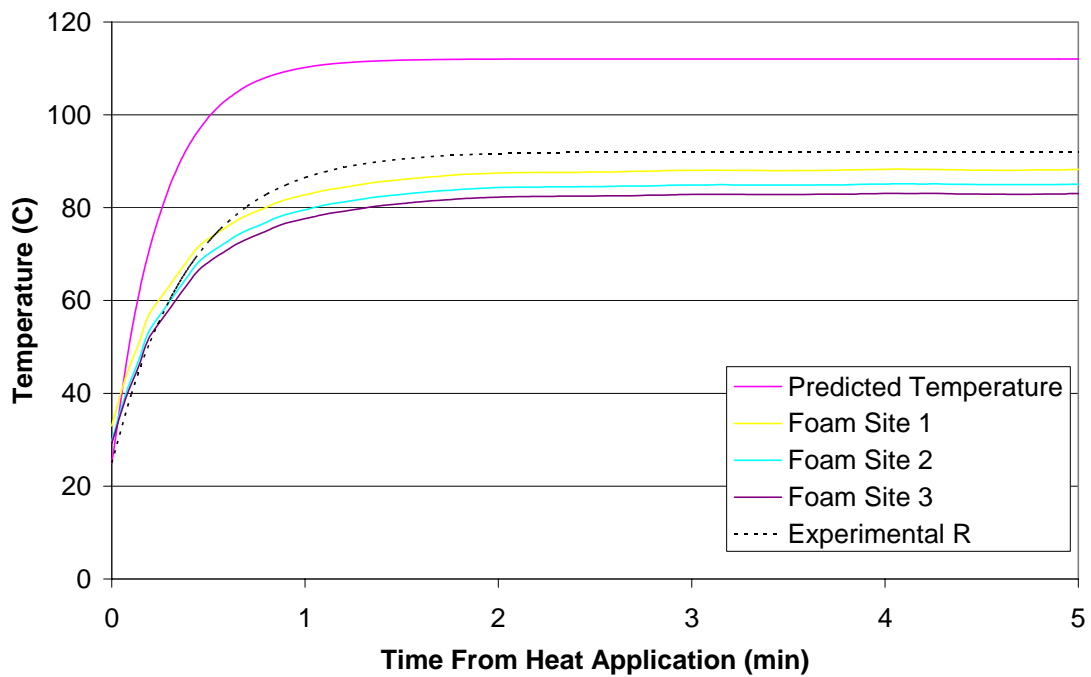
Predicted vs. Actual Temperature (Poco, Acetamide, Cooled, 135C)
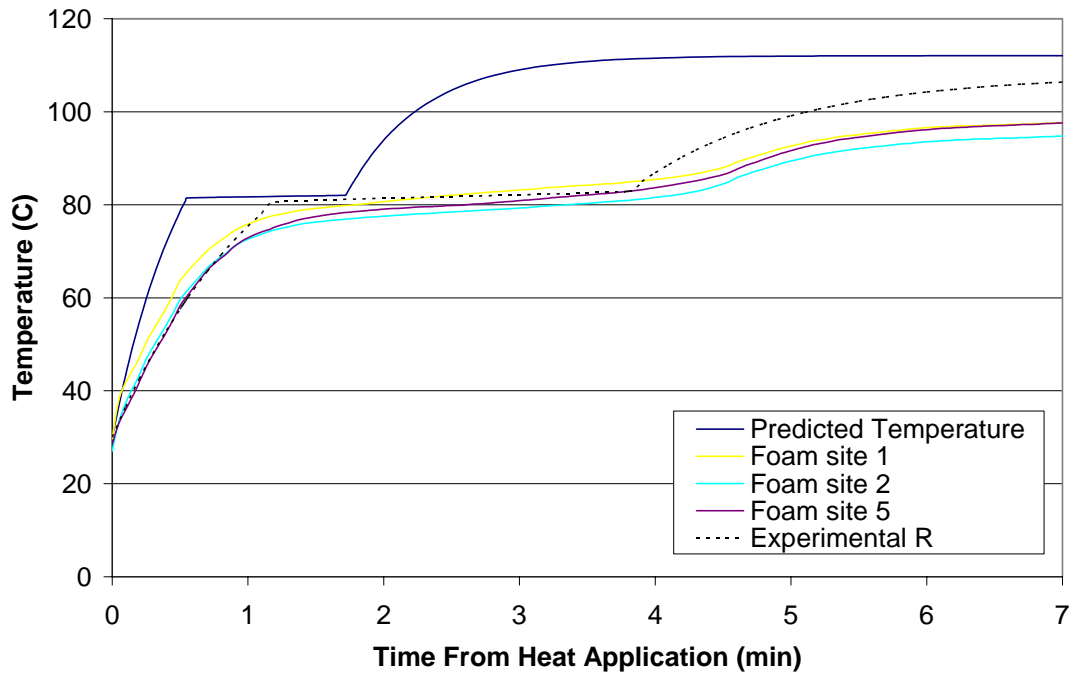
Predicted vs. Actual Temperature (Poco, Paraffin, Cooled, 95C)
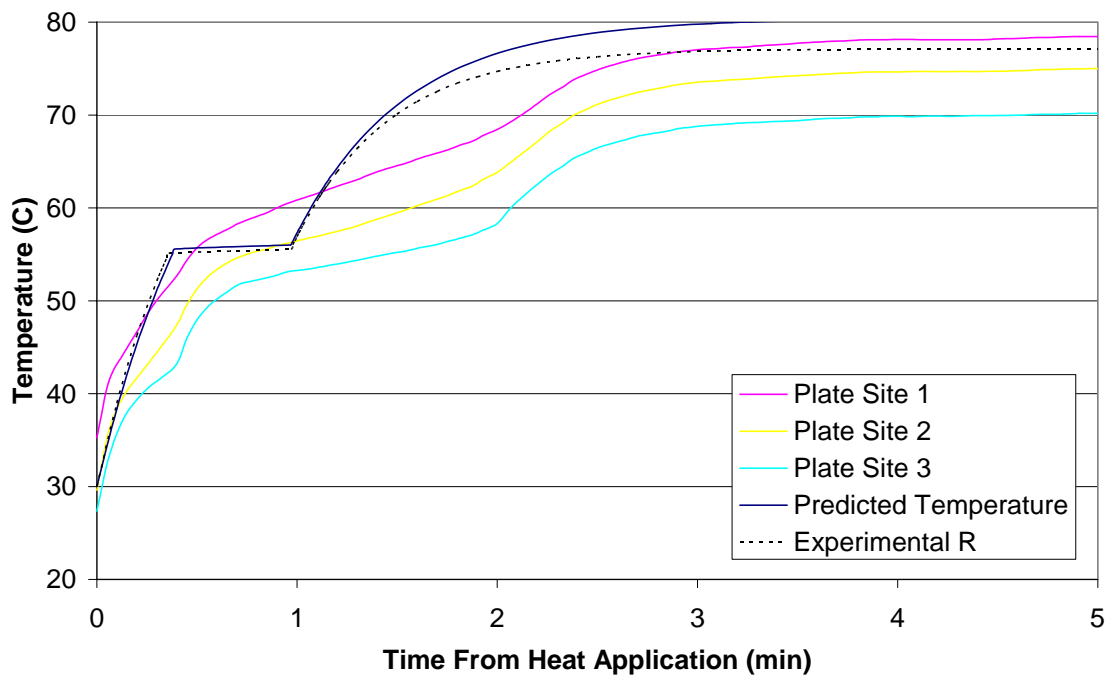
Appendix B: Power Charts

Predicted Vs. Actual Power into Foam (MER, Empty, Insulated, 70C)
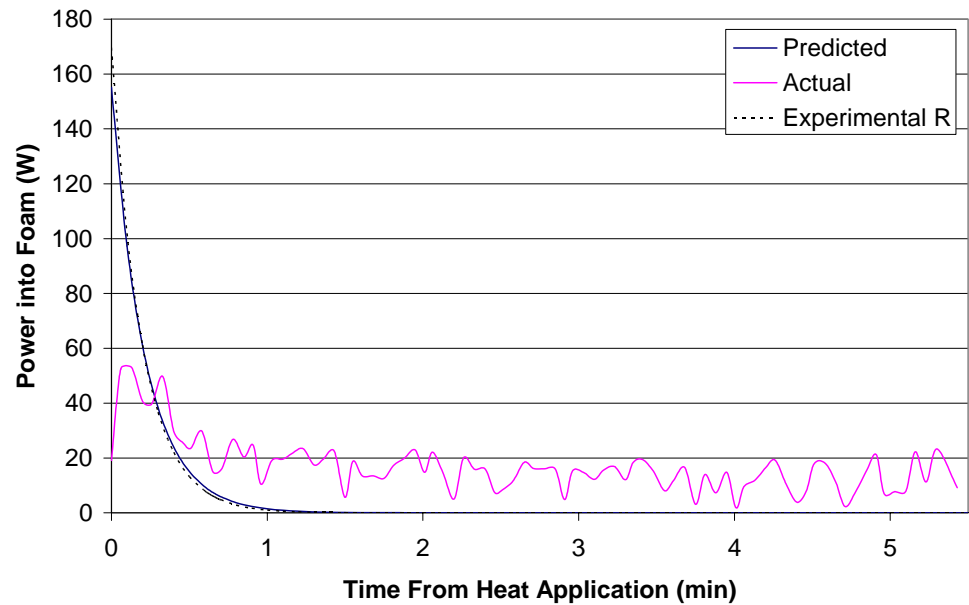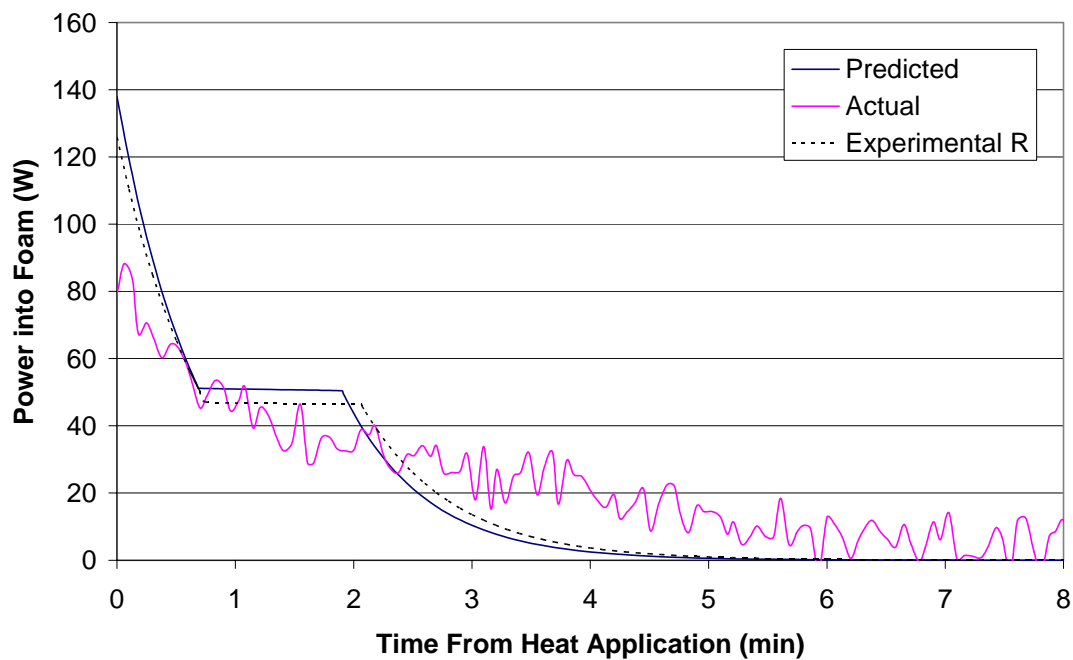

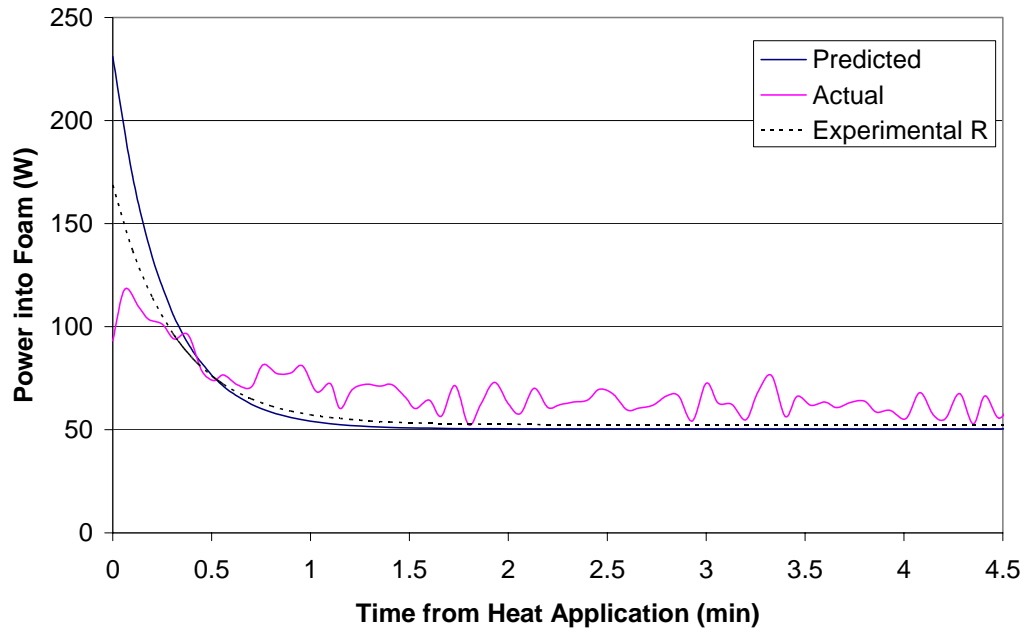**Predicted vs. Actual Power into Foam (MER , Empty, Insulated, 95C)**
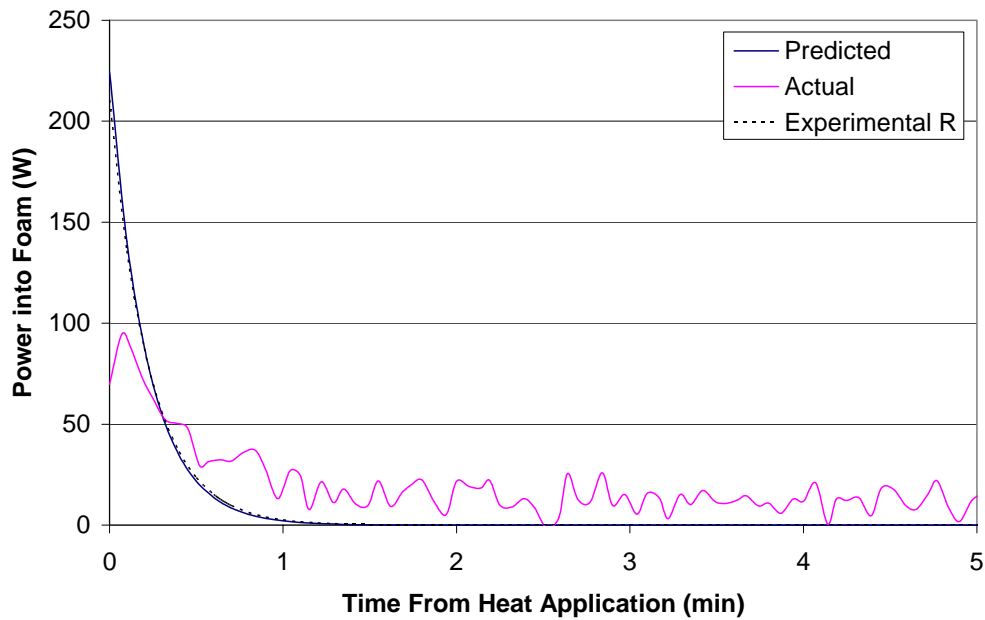
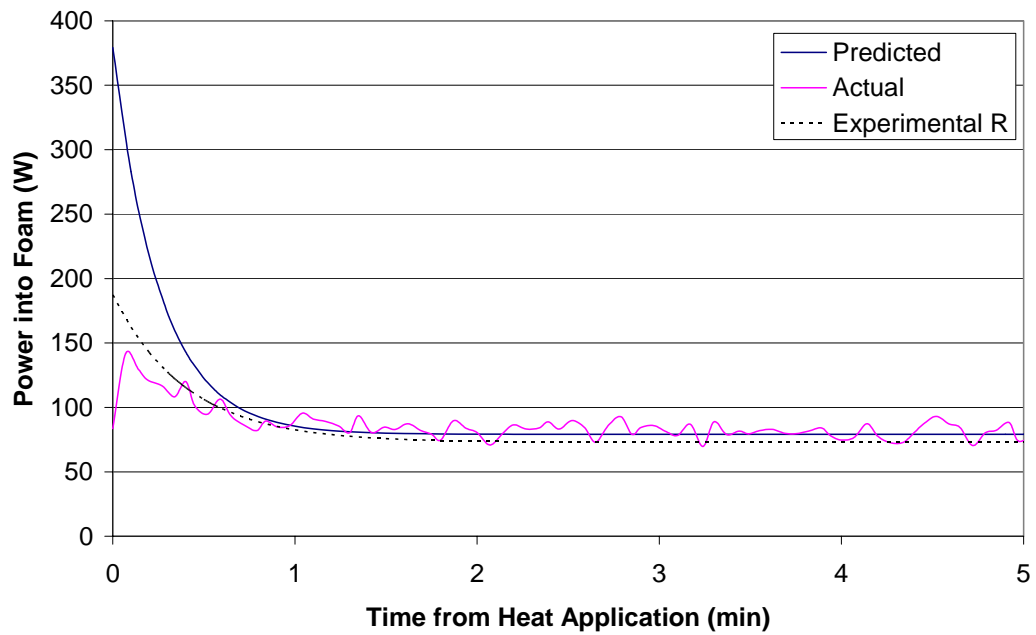**Predicted vs. Actual Power into Foam (MER, Acetamide, Insulated, 95C)**
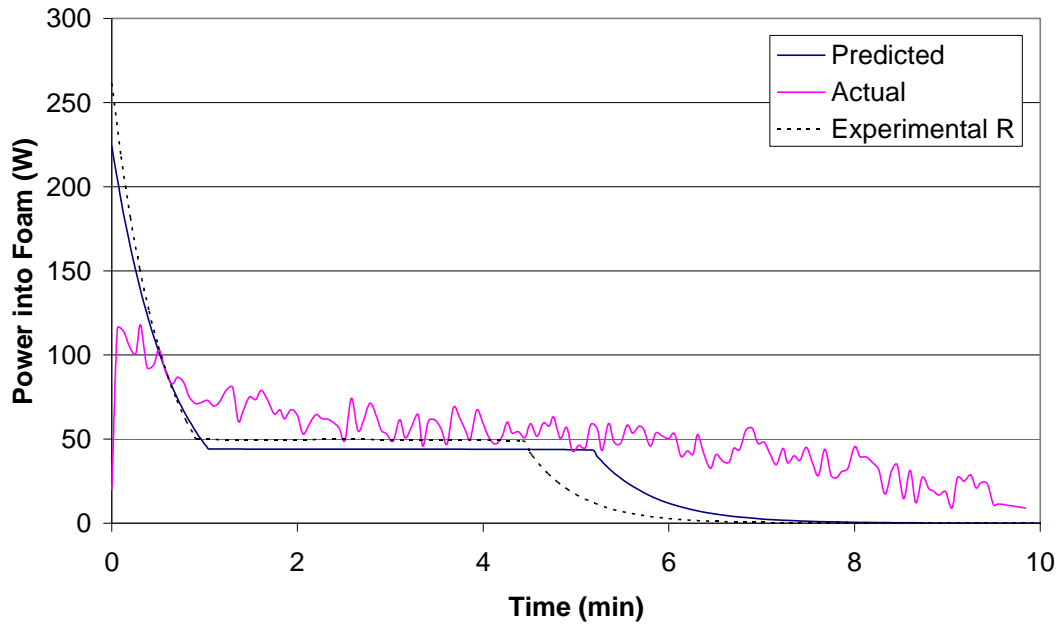
Predicted vs. Actual Power into Foam (MER, Paraffin, Insulated, 70C)
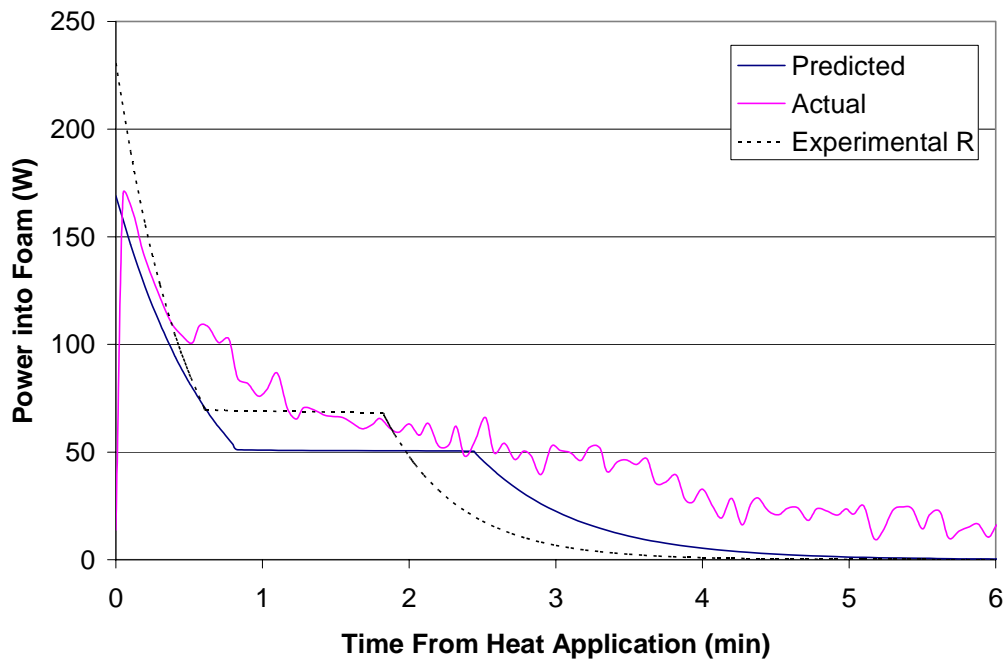
Predicted vs. Actual Power into Foam (MER, Empty, Cooled, 95C)
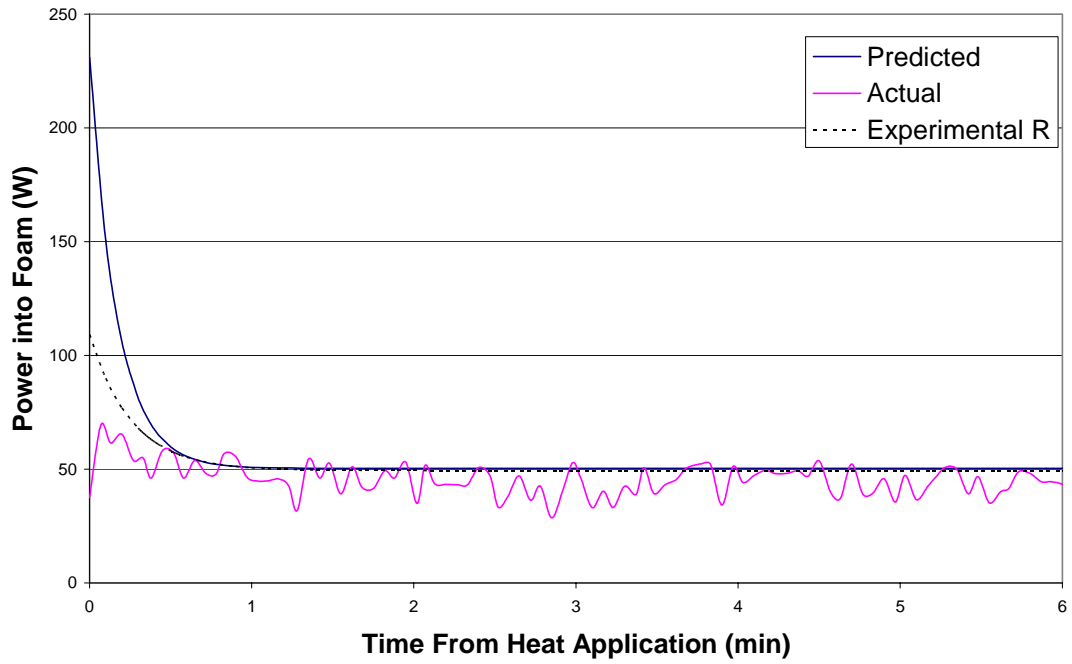
Predicted vs. Actual Power into Foam (MER, Empty, Cooled 135C)
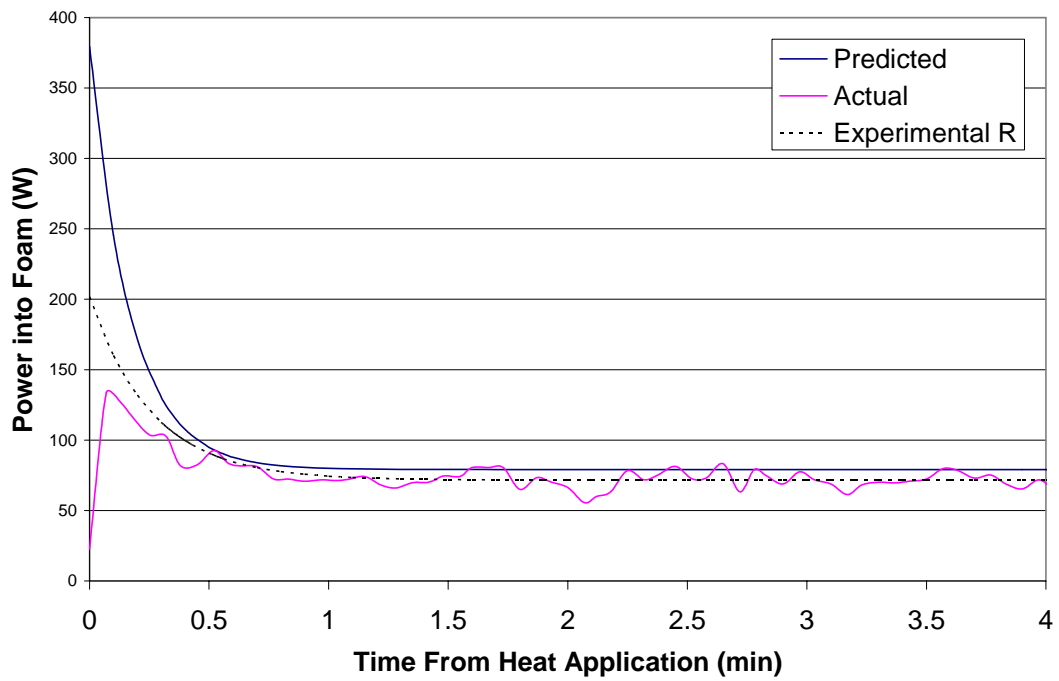
Predicted vs. Actual Power into Foam (MER, Acetamide, Cooled, 135C)
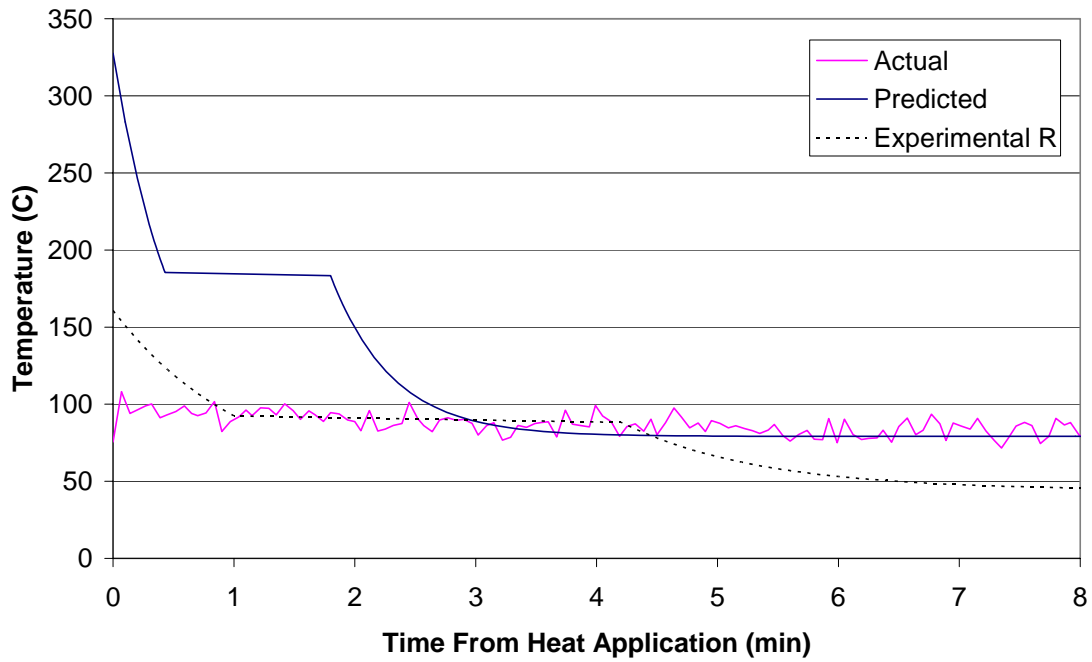
Predicted vs. Actual Power into Foam (MER, Paraffin, Cooled, 95C)

Predicted vs. Actual Power into Foam (Poco, Empty, Insulated, 70C)

Predicted vs. Actual Power into Foam (Poco, Empty, Insulated, 95C)

Predicted vs. Actual Power into Foam (Poco, Acetamide, Insulated, 95C)

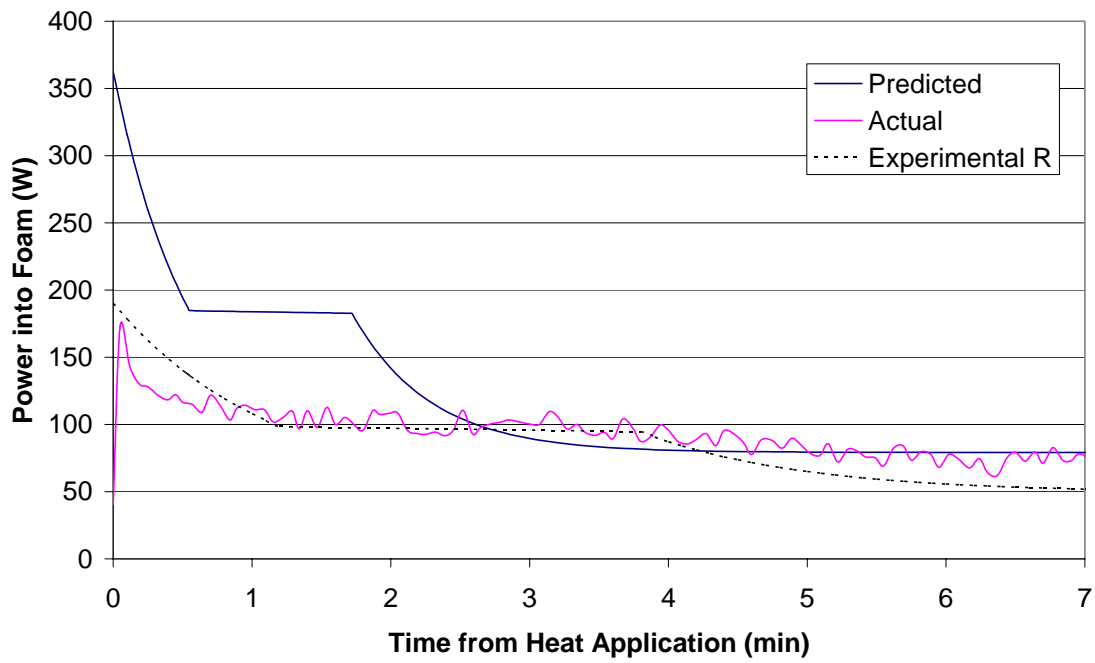**Predicted vs. Actual Power into Foam (Poco, Paraffin, Insulated, 70C)**

49

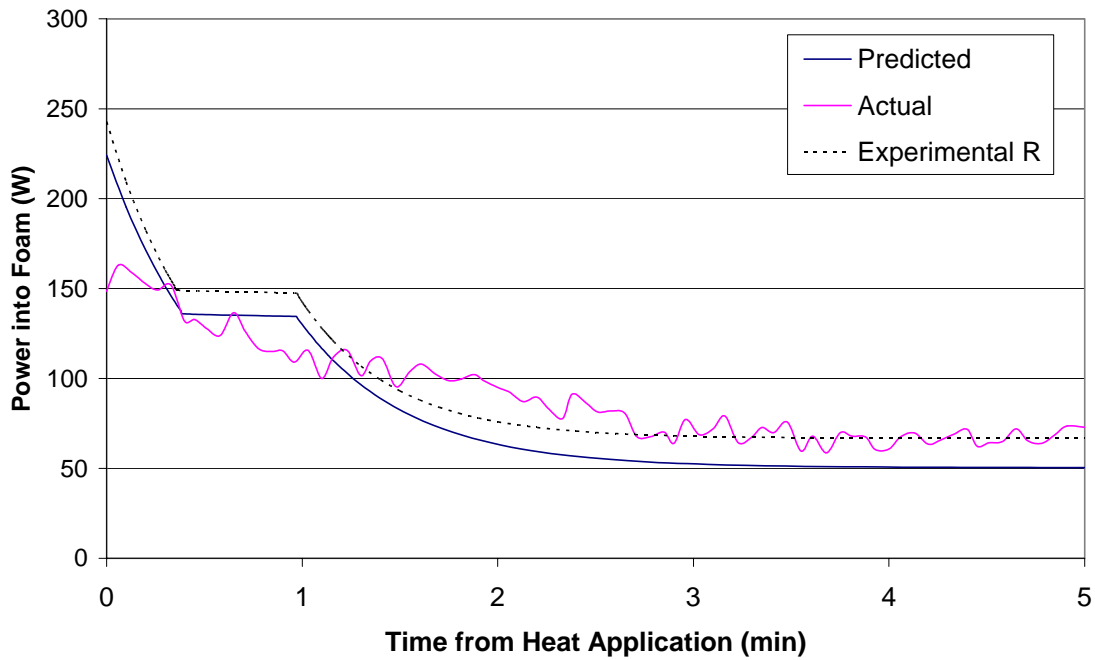**Predicted vs. Actual Power into Foam (Poco, Empty, Cooled, 95C)**

Predicted vs. Actual Power into Foam (Poco, empty, cooled, 135C)

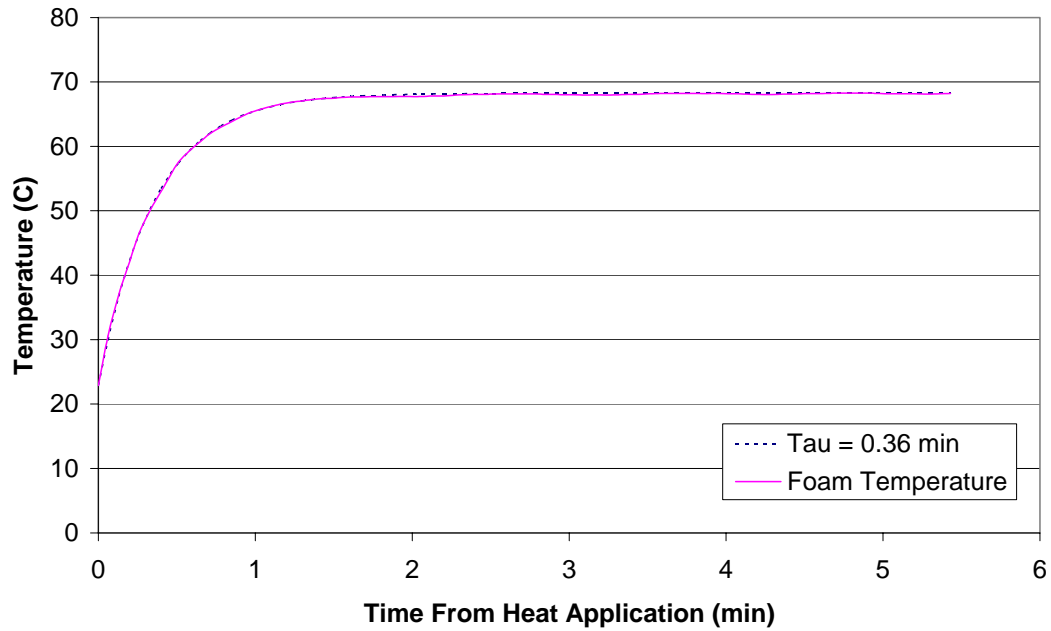## Predicted vs. Actual Power into Foam (Poco, Acetamide, Cooled, 135C)

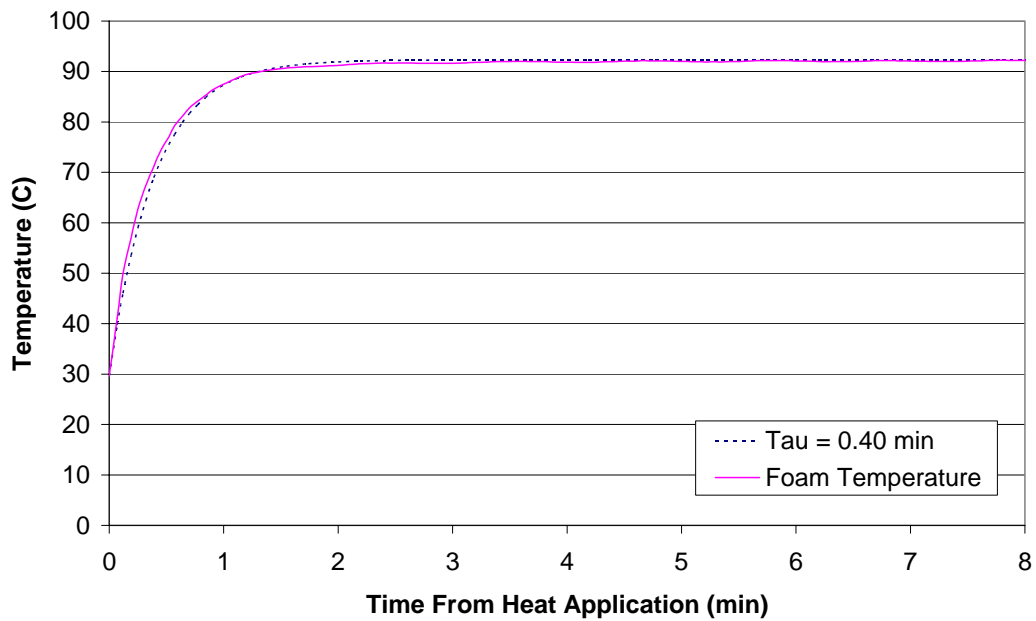## Predicted vs. Actual Power into Foam (Poco, Paraffin, Cooled, 95C)
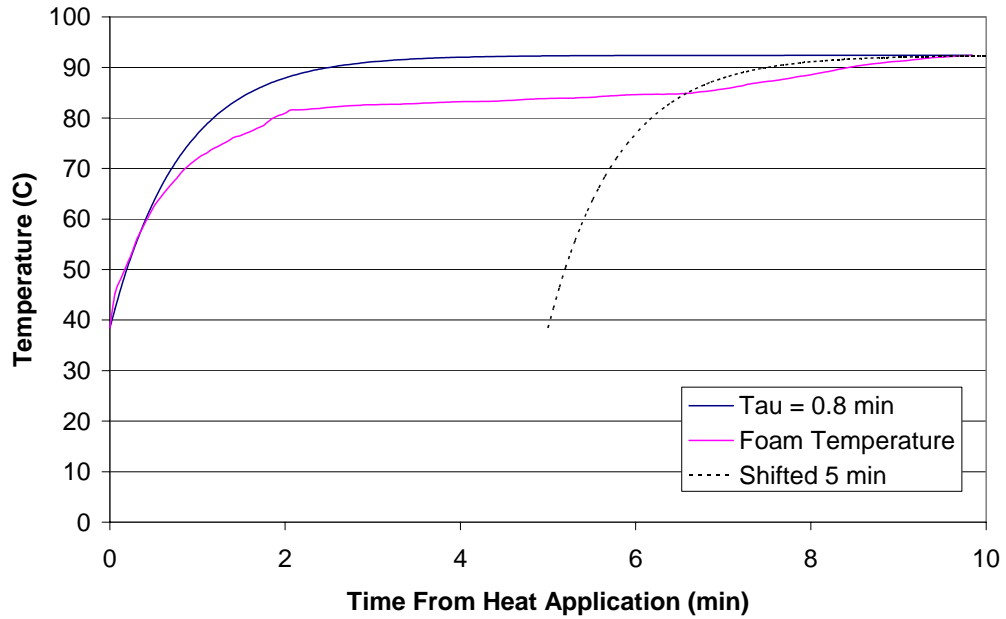
Appendix C: Curve Fit Charts
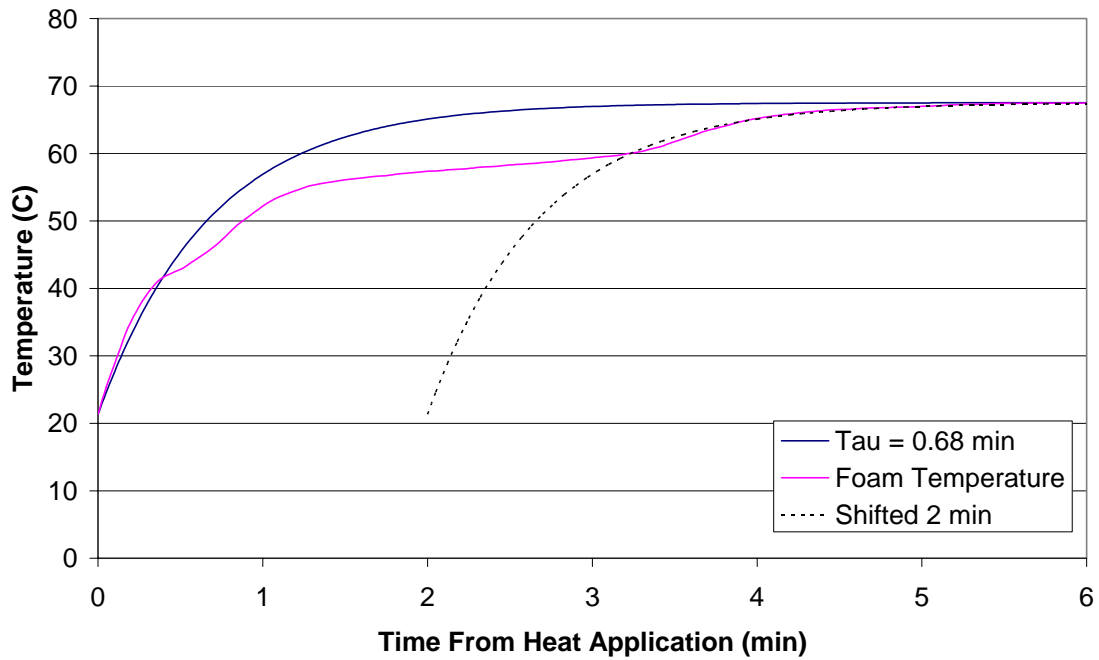
Time Constant (MER, Empty, Insulated, 70C)
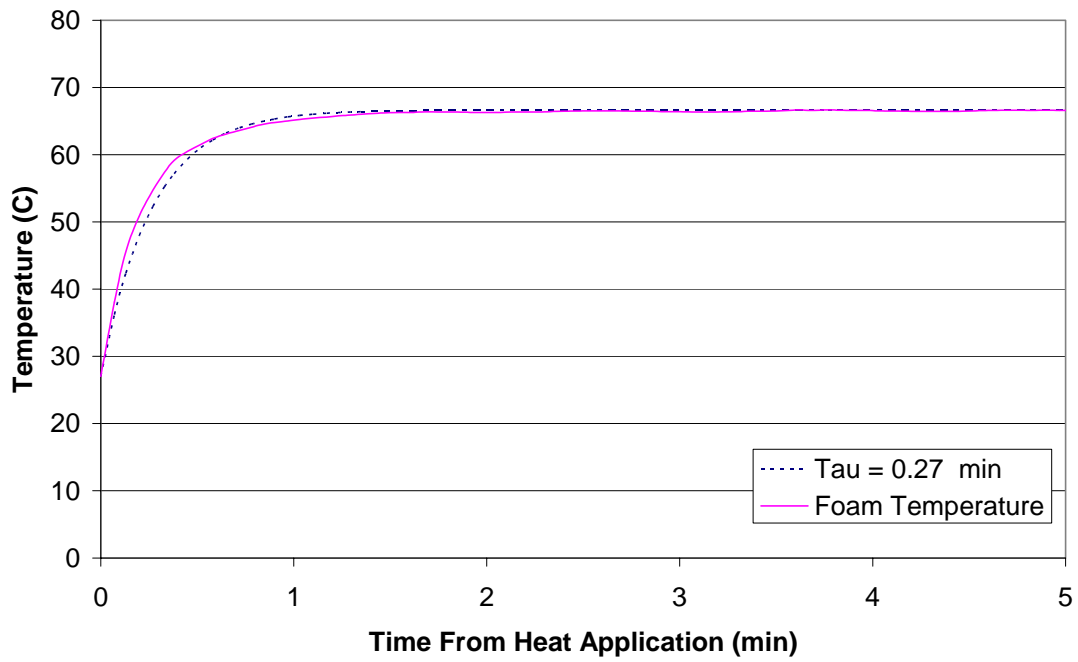

Time Constant (MER, Empty, Insulated, 95C)

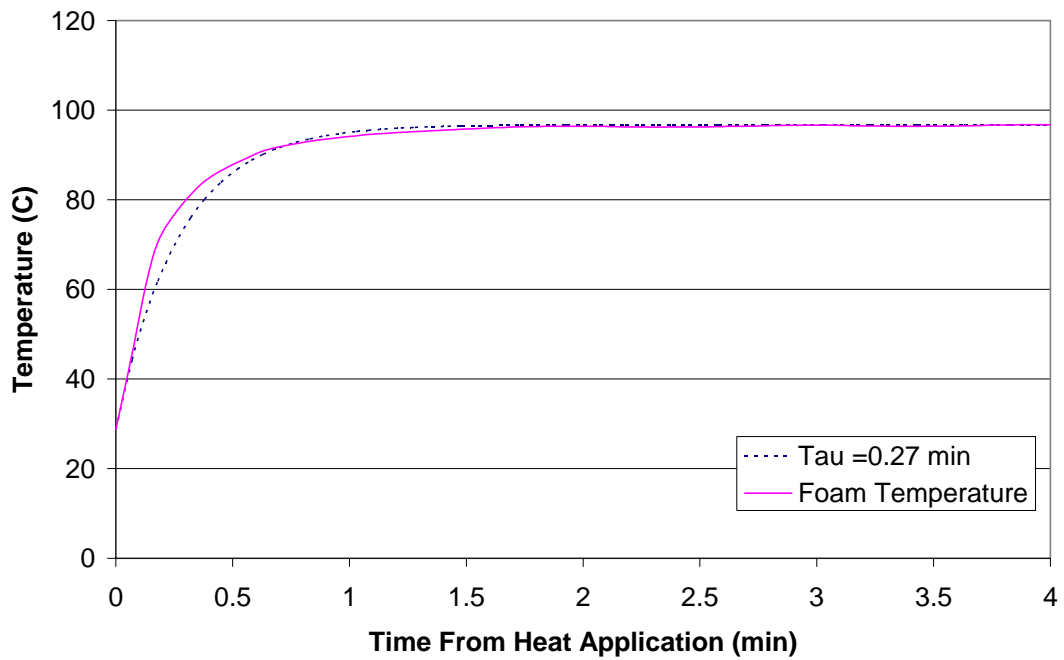## Time Constant (MER, Acetamide, Insulated, 95C)

Time Constant (MER, Paraffin, Insulated, 70C)

Time Constant (MER, Empty, Cooled, 95C)

Time Constant (MER, Empty, Cooled, 135C)

Time Constant (MER, Acetamide, Cooled, 135C)

Time Constant (MER, Paraffin, Cooled, 95C)

Time Constant (Poco, Empty, Insulated, 70C)

Time Constant (Poco, Empty, Insulated, 95C)

56

Time Constant (Poco, Acetamide, Insulated, 95C)

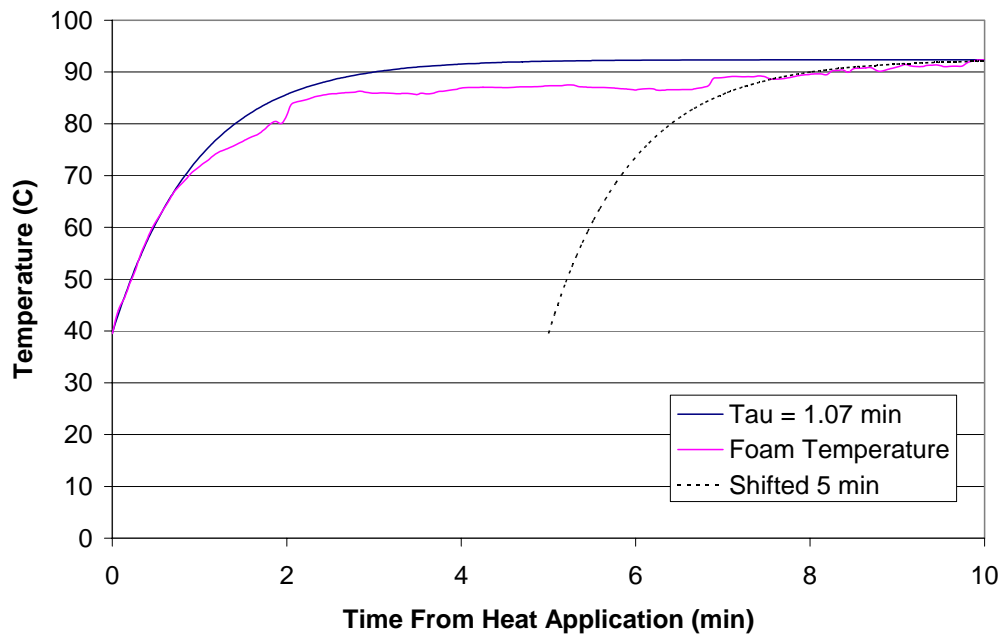**Time Constant (Poco, Paraffin, Insulated, 70C)**

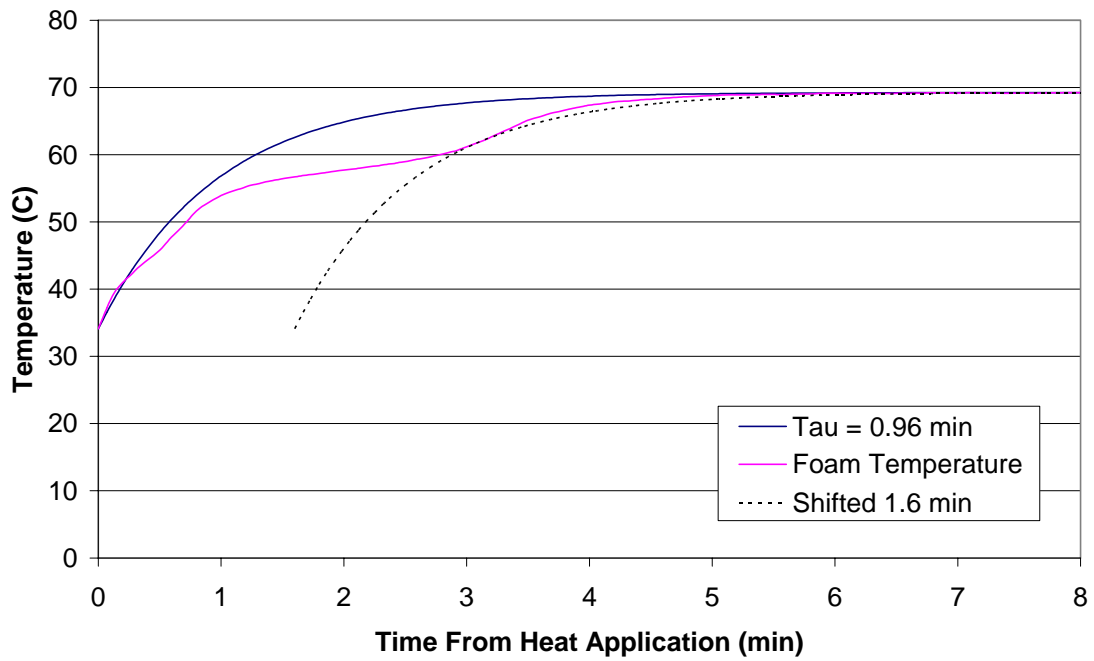**Time Constant (Poco, Empty, Cooled, 95C)**
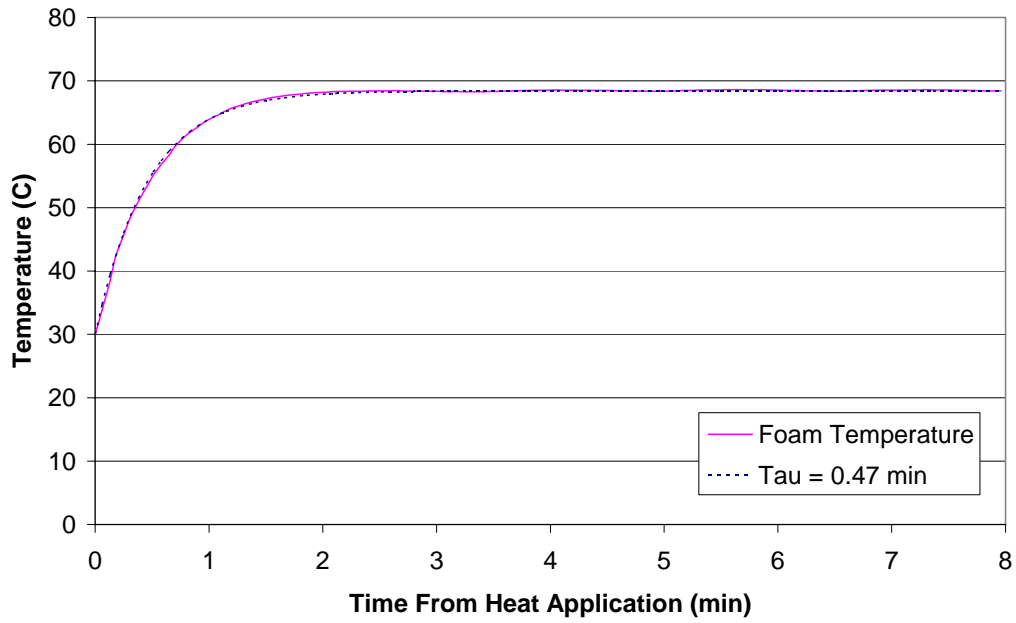

Time Constant (Poco, Empty, Cooled, 135C)
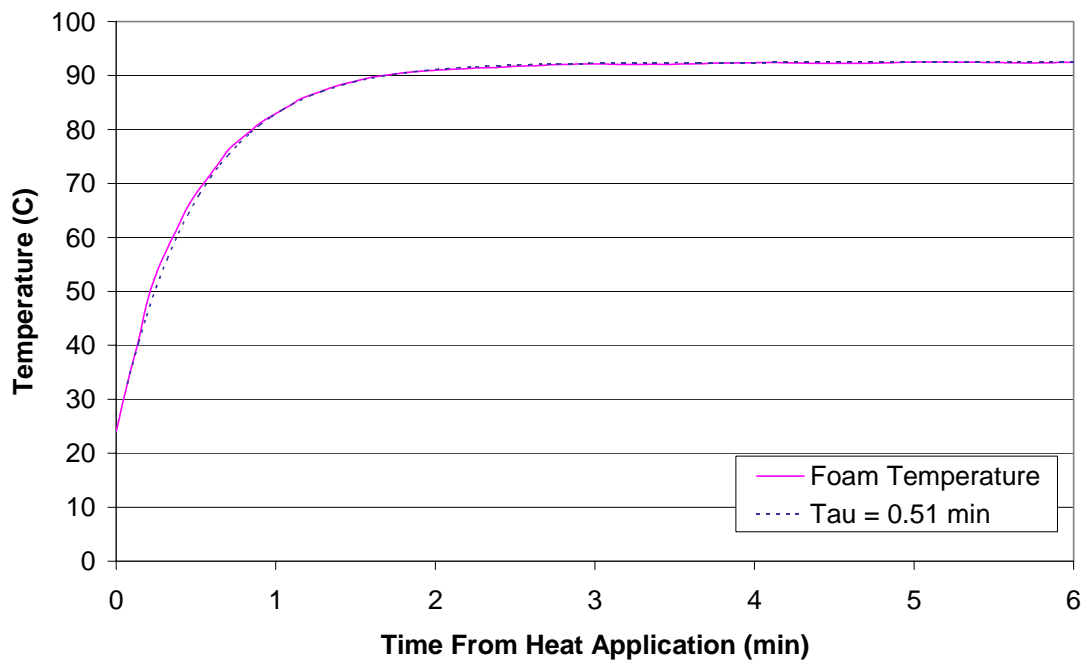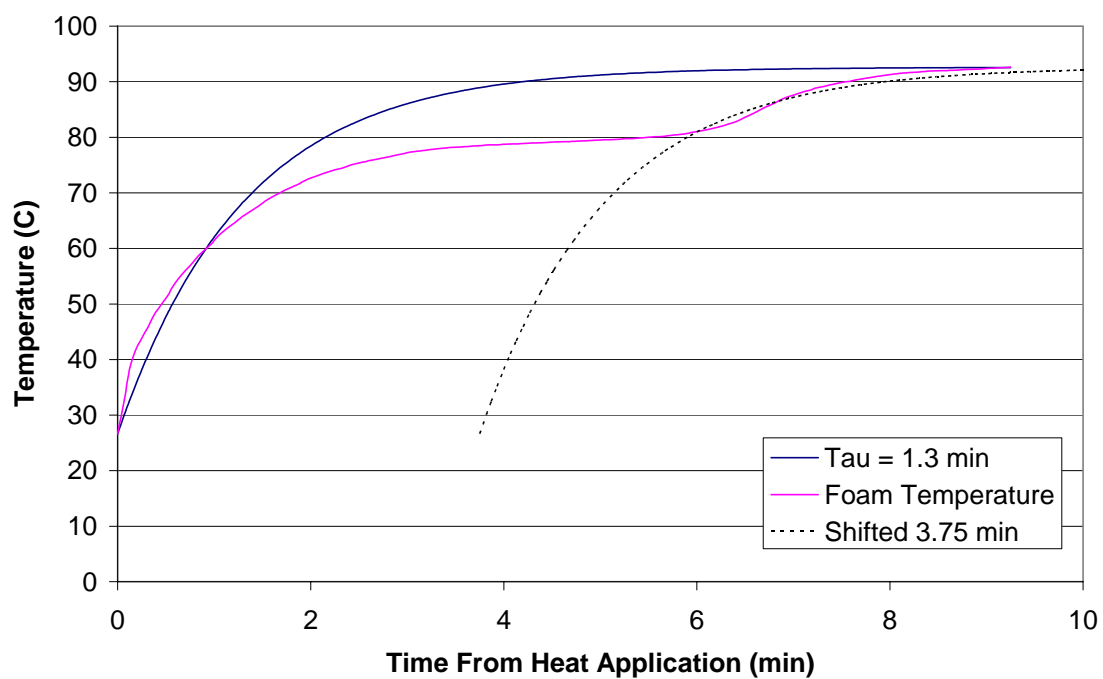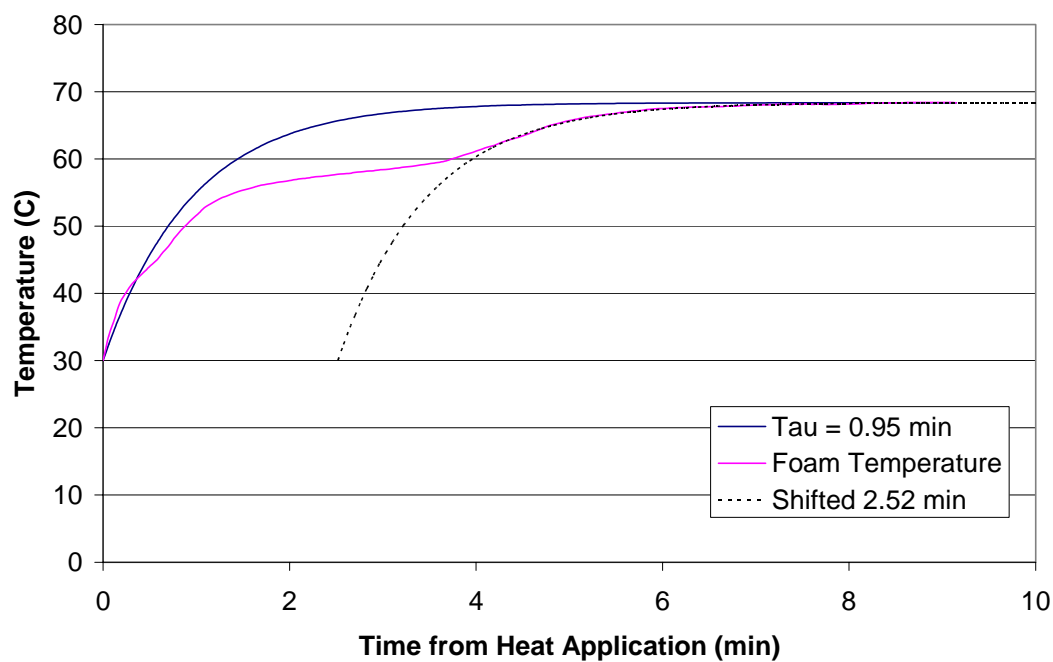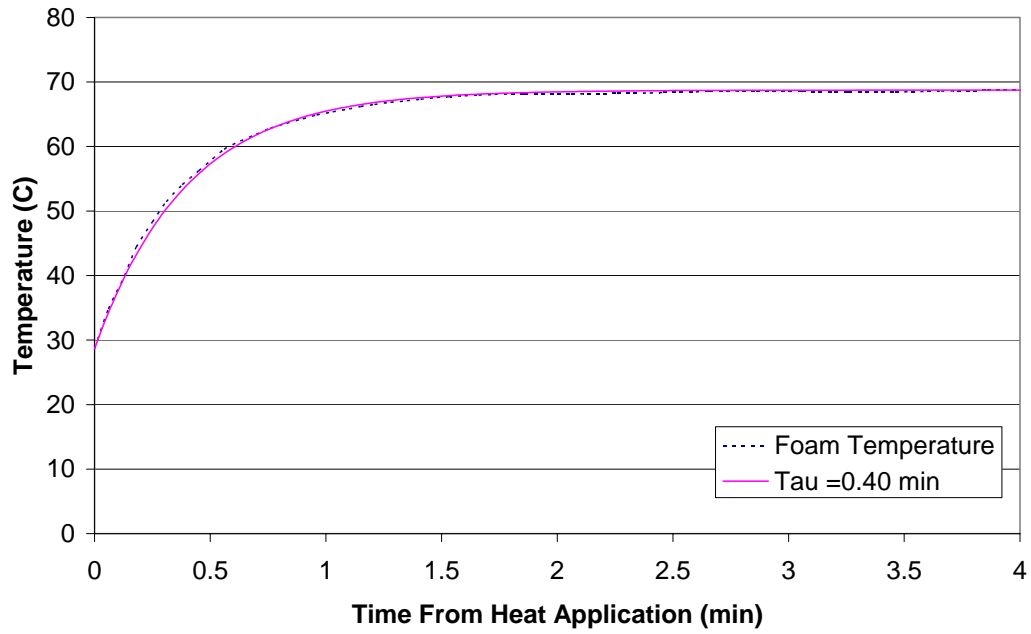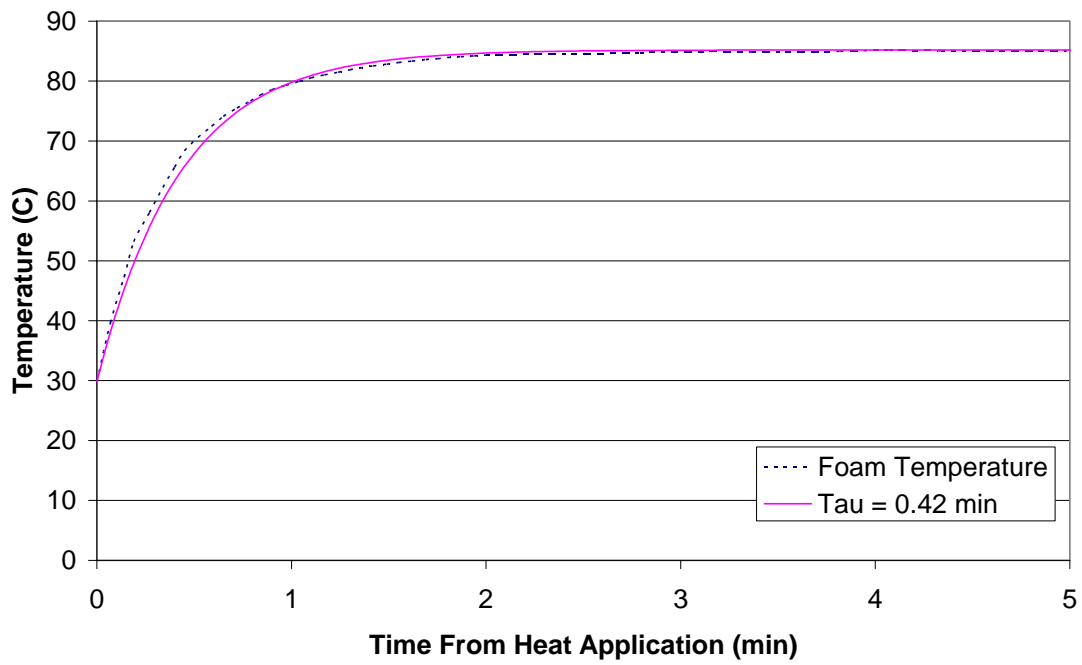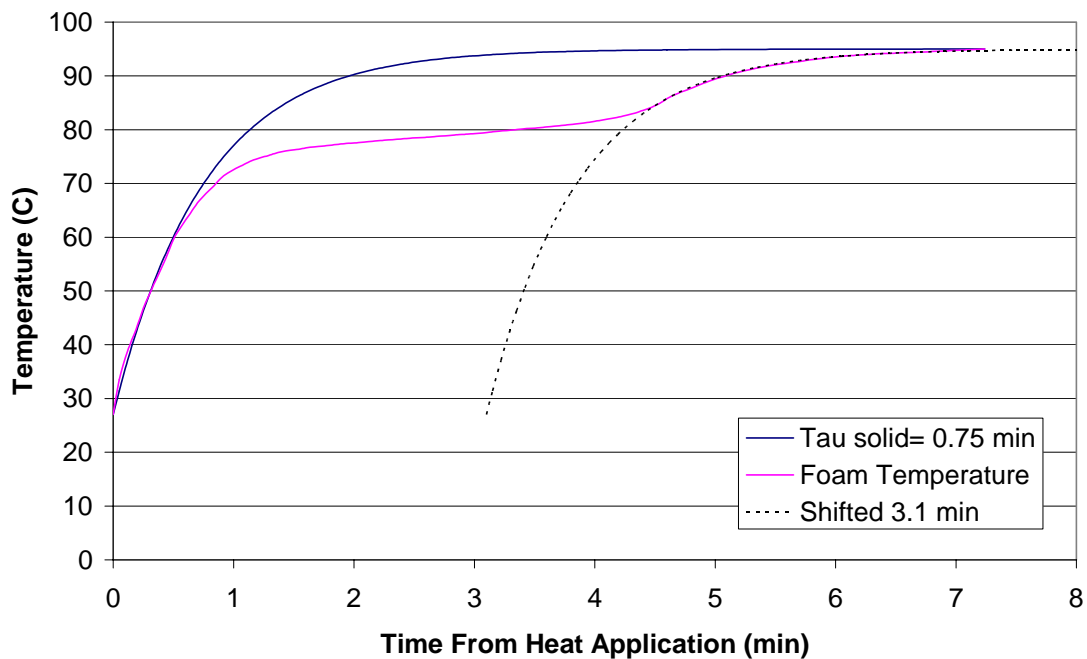
Time Constant (Poco, Acetamide, Cooled, 135C)

Time Constant (Poco, Paraffin, Cooled, 95C)

59
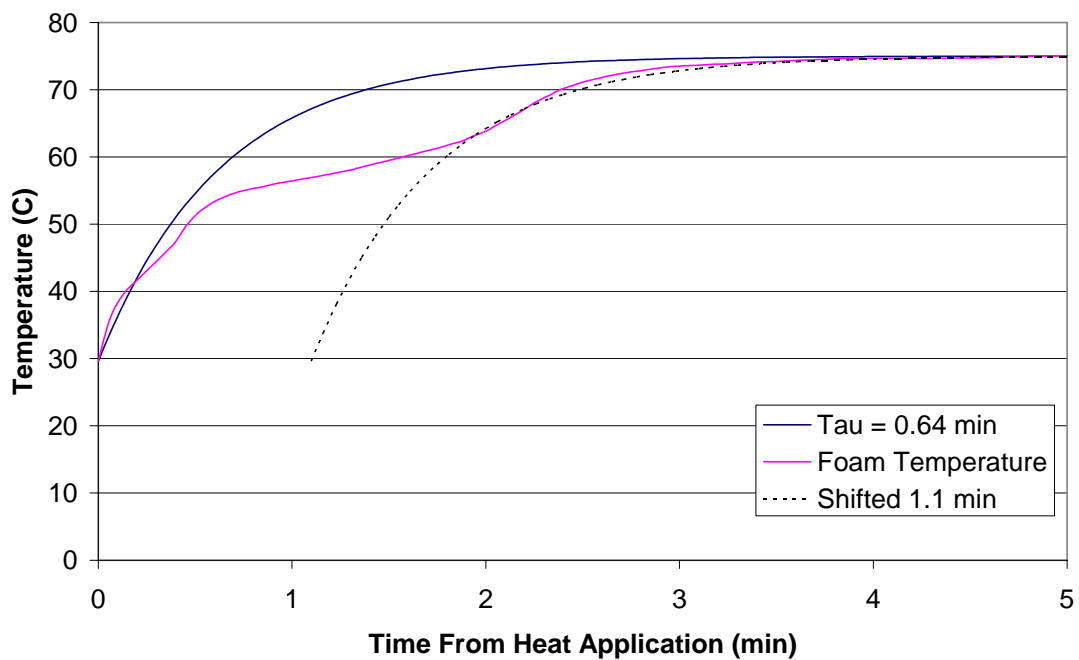
Appendix D: Sample Calculations for Time Constant

This section shows a sample calculation to determine the time constant of the Poco, cooled, acetamide, 135° C scenario.

Given:

$$T = \frac{R_C \cdot T_H + R_H \cdot T_C}{R_C + R_H} + \left(T_i - \frac{R_C \cdot T_H + R_H \cdot T_C}{R_C + R_H} \right) \cdot e^{-\left(\frac{R_C + R_H}{R_C \cdot R_H \cdot (M_f \cdot c_f + M_{PCM} \cdot c_{PCM})} \right) \cdot t}$$

$$R_H = R_{copper} + R_{grease} + R_{ccplate} + R_{bond} + R_{foam}$$

$$R_C = R_{foam} + R_{bond} + R_{ccplate} + R_{grease} + R_{final}$$

R_{grease}=0.03 (C/W)   (1:1)
R_{final}=0.81 (C/W)   (5:2)
T_H= 135° C   boundary condition
T_C= 25° C   boundary condition
$T_{initial}$= 30° C   initial condition
M_f= 60.09g   measured
M_{PCM}=38.95g   measured
c_{carbon}=1.1715 (J/g*K)   (13:Table 2)
$c_{acetamide}$= 1.98 (J/g*K)   (4:483-490)

	k (W/mK)	L (m)	A (m^2)
Copper	397.5	0.00127	0.00213
Foam	240	8.89*10^{-4}	0.00213
Carbon-carbon plate	3	7.79*10^{-4}	0.00213
Bond	0.88	2.54*10^{-4}	0.00213

k copper from (2:6-69), k foam and carbon-carbon plate from(AFRL), k bond from(7:831)

Solution:
Solving for the resistance network resistances

$$R_{copper} = \frac{L}{k \cdot A} = \frac{0.00127m}{397.5\left(\frac{W}{mK}\right) \cdot 0.00213m^2} = 0.0014\left(\frac{K}{W}\right) = 0.0014\left(\frac{C}{W}\right)$$

$$R_{foam} = \frac{L}{k \cdot A} = \frac{8.89 \cdot 10^{-4}\,m}{240\left(\dfrac{W}{mK}\right) \cdot 0.00213m^2} = 0.0017\left(\frac{K}{W}\right) = 0.0017\left(\frac{C}{W}\right)$$

$$R_{ccplate} = \frac{L}{k \cdot A} = \frac{7.79 \cdot 10^{-4}\,m}{3\left(\dfrac{W}{mK}\right) \cdot 0.00213m^2} = 0.1219\left(\frac{K}{W}\right) = 0.1219\left(\frac{C}{W}\right)$$

$$R_{bond} = \frac{L}{k \cdot A} = \frac{2.54 \cdot 10^{-4}\,m}{0.88\left(\dfrac{W}{mK}\right) \cdot 0.00213m^2} = 0.137\left(\frac{K}{W}\right) = 0.137\left(\frac{C}{W}\right)$$

These resistances then sum to for the values of R_H and R_C

$$R_H = 0.0014 + 0.03 + 0.1219 + 0.137 + 0.0017 = 0.29\left(\frac{K}{W}\right)$$

$$R_C = 0.0017 + 0.137 + 0.1219 + 0.03 + 0.81 = 1.1\left(\frac{K}{W}\right)$$

Substituting back into the equation for the temperature

$$T = \frac{1.1\left(\dfrac{C}{W}\right) \cdot 135C + 0.29\left(\dfrac{C}{W}\right) \cdot 25C}{1.1\left(\dfrac{C}{W}\right) + 0.29\left(\dfrac{C}{W}\right)}$$
$$+ \left(30C - \frac{1.1\left(\dfrac{C}{W}\right) \cdot 135C + 0.29\left(\dfrac{C}{W}\right) \cdot 25C}{1.1\left(\dfrac{C}{W}\right) + 0.29\left(\dfrac{C}{W}\right)} \right) \cdot e^{\left(\frac{1.1\left(\frac{C}{W}\right)+0.29\left(\frac{C}{W}\right)}{1.1\left(\frac{C}{W}\right) \cdot 0.29\left(\frac{C}{W}\right) \cdot \left(60.09g \cdot 1.1715\left(\frac{J}{gC}\right) + 38.95g \cdot 1.98\left(\frac{J}{gC}\right)\right)} \right) \cdot t}$$

Simplifying the equation for the temperature becomes

$$T = 112 - 82 \cdot e^{-(0.0295) \cdot t}$$

And τ becomes

$$\tau = \frac{1}{0.0295}\,s = 33.89s = 0.57\,\text{min}$$

Appendix E: Sample Calculation for Phase Change Time

Given:

$$t_{pha\sec hange} = \frac{M \cdot h_{sf}}{q_{in} - \sum q_{out}}$$

$$q = \frac{T - T_f}{R}$$

R_H=0.29 (C/W)	solved for in Appendix D
R_C=1.1 (C/W)	solved for in Appendix D
T_H=135° C	boundary condition
T_C=25° C	boundary condition
$T_{melt} = 81°$ C	(6:Table 5-2)
$h_{sf} = 241$ (J/g)	(6: Table 5-2)
M_{PCM}=38.05 g	measured

Glass insulation
      $k(81°$ C$) = 0.0712$ (W/mK)   (7:835)
      thickness $= 0.00635$ m   measured

Sample dimensions
      Length $= 0.0555$ m   measured
      Width $= 0.0381$ m   measured
      Height $= 0.0285$ m   measured

Solution:

Solving for the q terms

$$q_{in} = \frac{T_H - T_{melt}}{R_H} = \frac{153C - 81C}{0.29\left(\frac{C}{W}\right)} = 186.2W$$

$$q_{out} = \frac{T_{melt} - T_C}{R_C} = \frac{81C - 25C}{1.1\left(\dfrac{C}{W}\right)} = 51W$$

Estimate losses out the sides

$$R_{loss} = \frac{L_{glass}}{k \cdot A} = \frac{0.00635m}{0.0712(W/mK) \cdot (2 \cdot (0.0555m + 0.0381m) \cdot 0.0285m)} = 16.7\left(\frac{K}{W}\right)$$

$$q_{loss} = \frac{T_{melt} - T_C}{R_{loss}} = \frac{81C - 25C}{16.7\left(\dfrac{K}{W}\right)} = 3.35W$$

Substituting these values for q into the equation for the time for the phase change

$$t_{phase\,change} = \frac{M \cdot h_{sf}}{q_{in} - \sum q_{out}} = \frac{38.05g \cdot 241\left(\dfrac{J}{g}\right)}{186.2W - 51W - 3.35W} = 69.5s = 1.16\min$$

Bibliography

1. *AAvid Ultrastick Phase-Change Thermal interface Compound.* Product Flyer. AAvid Thermalloy, no date.

2. Avallone, EugeneA. And Theodore Baumeister III. *Marks' Standard Handbook for Mechanical Engineers*, McGraw Hill, 1996.

3. Boas, Mary L. *Mathematical Methods in the Physical Sciences (Second Edition).* John Wiley and Sons, 1983.

4. Buddhi, D., S. D. Sharma, and R. L. Shawney. "Accelerated Thermal Cycle Test of Latent Heat Storage Materials," *Journal Solar Energy Engineering,* Vol 66 Issue 6, 1999.

5. Cao, Yiding and Rengasamy Ponnappan. "A Liquid Cooler Module with Carbon Foam for Electronics Cooling Applications," *42nd AIAA Aerospace Sciences Meeting and Exhibit*, p1216-1223, Reston: AIAA press, 2004.

6. Hale, D. V., M. J. Hoover, and M. J. O'Neil. *Phase Change Materials Handbook*, NASA CR-61363, September 1971.

7. Incropera, Frank P and David P. DeWitt. *Fundamentals of Heat and Mass Transfer (Fourth Edition).* John Wiley and Sons, 1996.

8. Klett, James. "High Thermal Conductivity Carbon Foam." http://www.ms.ornl.gov/researchgroups/cmt/foam/foams.htm. 25 October 2004.

9. Lee, C William and Khalid Lafdi. "Stabilization study of Carbon Foam," *SAMPE Technical Conference*, 29 Sept 2003.

10. McCoy, John W and Daniel L. Vrable. "Metal Matrix Composites from Graphitic Foams and Copper," *SAMPE Journal*, Vol 40 No 1, January/February 2004.

11. Hagar, Joseph W. and Max L. Lake. "Novel Hybrid Composites Based on Carbon Foams," *Materials Research Society Symposium Proceedings*, Vol 270, Pennsylvania, 1992.

12. "Poco Graphite – Thermal Management Materials." http://www.poco.com/thermal/foam.asp. 25 October 2004.

13. "Properties of Non-Metallic Solids." http://www.hotwatt.com/table2. 14 January 2005.

REPORT DOCUMENTATION PAGE				*Form Approved* *OMB No. 074-0188*

The public reporting burden for this collection of information is estimated to average 1 hour per response, including the time for reviewing instructions, searching existing data sources, gathering and maintaining the data needed, and completing and reviewing the collection of information. Send comments regarding this burden estimate or any other aspect of the collection of information, including suggestions for reducing this burden to Department of Defense, Washington Headquarters Services, Directorate for Information Operations and Reports (0704-0188), 1215 Jefferson Davis Highway, Suite 1204, Arlington, VA 22202-4302. Respondents should be aware that notwithstanding any other provision of law, no person shall be subject to an penalty for failing to comply with a collection of information if it does not display a currently valid OMB control number.
PLEASE DO NOT RETURN YOUR FORM TO THE ABOVE ADDRESS.

1. REPORT DATE *(DD-MM-YYYY)* 21-03-2005	**2. REPORT TYPE** **Master's Thesis**		**3. DATES COVERED** *(From – To)* 26-08-2004 – 21-03-2005

4. TITLE AND SUBTITLE Thermal Characteristics of Pitch Based Carbon Foam	**5a. CONTRACT NUMBER**
	5b. GRANT NUMBER
	5c. PROGRAM ELEMENT NUMBER
6. AUTHOR(S) Wierschke, Kevin W., Captain, USAF	**5d. PROJECT NUMBER**
	5e. TASK NUMBER
	5f. WORK UNIT NUMBER

7. PERFORMING ORGANIZATION NAMES(S) AND ADDRESS(S)
  Air Force Institute of Technology
 Graduate School of Engineering and Management (AFIT/EN)
 2950 Hobson Way
  WPAFB OH 45433-7765
	8. PERFORMING ORGANIZATION REPORT NUMBER
	
	 AFIT/GSS/ENY/05-M05

9. SPONSORING/MONITORING AGENCY NAME(S) AND ADDRESS(ES)
  AFRL/MLBC
  Attn: Mr. Roland Watts
 2941 Hobson Way
  WPAFB OH 45433-7765   DSN: 785-9067
	10. SPONSOR/MONITOR'S ACRONYM(S)

	11. SPONSOR/MONITOR'S REPORT NUMBER(S)

12. DISTRIBUTION/AVAILABILITY STATEMENT   APPROVED FOR PUBLIC RELEASE; DISTRIBUTION UNLIMITED.

13. SUPPLEMENTARY NOTES

14. ABSTRACT

        Phase-change thermal energy storage devices offer thermal control systems an option that allows a smaller heat sink to be used by absorbing the thermal energy quickly and storing it in the phase change to prevent failure of electronic components and then slowly releasing the heat to the heat sink. This paper experimentally determined the transient response of carbon foam with a phase-change material by measuring the response to a step temperature input to test samples. The transient response was recorded until steady state was reached. An analytic response was created and compared against the measured response. A simplified analytic prediction of the transient response was developed by using an energy balance. This approximation was then compared against the experimental results.

15. SUBJECT TERMS   Carbon foam, phase-change material, transient thermal response

16. SECURITY CLASSIFICATION OF:			**17. LIMITATION OF ABSTRACT**	**18. NUMBER OF PAGES**	**19a. NAME OF RESPONSIBLE PERSON** Milton Franke
REPORT **U**	**ABSTRACT** **U**	**c. THIS PAGE** **U**	**UU**	76	**19b. TELEPHONE NUMBER** *(Include area code)* (937) 255-3636, ext 4720; e-mail: milton.franke @afit.edu